universität wien

MASTERARBEIT / MASTER'S THESIS

Titel der Masterarbeit / Title of the Master's Thesis

"Influence of water quality parameters on methane ebullition emissions in the reed belt of Lake Neusiedl, Austria"

verfasst von / submitted by
Daniela Alejandra Henry Pinilla

angestrebter akademischer Grad / in partial fulfilment of the requirements for the degree of
Master of Science (MSc)

Wien, 2021 / Vienna, 2021

Studienkennzahl lt. Studienblatt / degree programme code as it appears on the student record sheet:	UA 066 299
Studienrichtung lt. Studienblatt / degree programme as it appears on the student record sheet:	Interdisziplinäres Masterstudium Environmental Sciences
Betreut von / Supervisor:	Univ.-Prof. Dipl.-Geogr. Dr. Stephan Glatzel

Acknowledgments

First of all, I would like to thank the Department of Geography and Regional Research from the University of Vienna for giving me the opportunity to be part of this project. I am very grateful of my teacher and supervisor Stephan Glatzel, who offered me without hesitation a space in his work group and supported my ideas with enthusiasm. Special thanks to Pamela Baur, PhD student of the department, for all the time she spent with me answering my thousand questions, for being empathic and supportive with my project and for the good/hard moments we shared in the field and in the lab. My gratitude to every one in this working group who shared with me a piece of knowledge, advice or just a nice conversation.

Last but not least, I would like to thank my family, in particular my mother for her unconditional support and my boyfriend for getting so involved in my project that he helped me in every stage of it, he worked hard with me on the field, helped me in my marathonic 12 hours measurements in the lab, discussed my struggles, celebrated my progress and read my thesis from the begging to the end. I could not have done it without you.

Abstract

Methane ebullition emissions might contribute significantly to greenhouse gas emissions from freshwater bodies, it might even be the most important pathway in some cases, specially in shallow lakes. Ebullition emission is not often estimated because of the high uncertainty of the episodic releases. This study provides an estimation of such emissions in a steppe lake in East-Austria, Lake Neusiedl. Weekly measurements were carried out during 15 weeks using ebullition traps in three different locations with nine sampling points at each one of them, obtaining methane ebullition fluxes that on average varied from 50.2 to 34 064.6 $\mu g\ CH_4\ m^{-2}d^{-1}$ depending on the location. At the same time, several water quality parameters were measured and then compared with methane concentration from the collected gas. The statistical analysis showed that the parameters which had the highest correlation with methane concentrations when looking at the whole data set were water depth, carbon, total nitrogen and electrical conductivity. When looking at each location separately were redox potential and water depth. Additionally, methane diffusion estimations ranged between 6 154.5 and 10 205.7 $\mu g\ CH_4\ m^{-2}d^{-1}$ depending on the location, while carbon dioxide and nitrous oxide varied from 839.5 to 901.0 and 1.1 to 12.5 $\mu g\ CH_4\ m^{-2}d^{-1}$, respectively.

Kurzfassung

Methan-Ebullitionsemissionen können erheblich zu den Treibhausgasemissionen aus Binnengewässer beitragen. In einigen Fällen, insbesondere in flachen Seen, können Ebullitionsemissionen den größten Emissionspfad darstellen. Aufgrund hoher Schwankungen der episodischen Freisetzung werden Ebullitionsemissionen nicht häufig geschätzt. Diese Studie liefert eine Schätzung der Methan-Ebullitionsemissionen des Neusiedler See, einem Steppensee in Ostösterreich. Wöchentliche Messungen wurden 15 Wochen lang mit Hilfe von Ebullitionsfallen an drei verschiedenen Standorten mit jeweils neun Probenahmestellen durchgeführt. Dabei wurden Methan-Ebullitionsflüsse ermittelt, die je nach Standort im Durchschnitt bei zwischen 50.2 und 34 064.6 $\mu g\ CH_4\ m^{-2}d^{-1}$ lagen. Gleichzeitig wurden mehrere Wasserqualitätsparameter gemessen und mit der Methankonzentration des gesammelten Gases verglichen. Die statistische Analyse ergab, dass die Parameter, die bei Betrachtung des gesamten Datensatzes die höchste Korrelation mit der CH4-Konzentration aufwiesen, Wassertiefe, Kohlenstoff, Gesamtstickstoff und elektrische Leitfähigkeit waren. Bei getrennter Betrachtung der einzelnen Standorte wiesen das Redoxpotenzial und die Wassertiefe die höchste Korrelation mit der Methan-Konzentration auf. Darüber hinaus lagen die Schätzungen für die Methandiffusion je nach Standort zwischen 6 154.5 und 10 205.7 $\mu g\ CH_4\ m^{-2}d^{-1}$, während Kohlendioxid und Distickstoffoxid zwischen 839.5 und 901.0 bzw. 1.13 und 12.50 $\mu g\ CH_4\ m^{-2}d^{-1}$ schwankten.

Table of Contents

List of Tables

List of Figures

List of Abbreviations

NH_4Cl	Ammonium chloride
$App.$	Approximately
$HCO_3{}^-$	Bicarbonate ion
CO_3^{-2}	Carbonate ion
CH	Channel
CH_4	Methane
CO_2	Carbon dioxide
DOY	Day of the year
DOC	Dissolved organic carbon
DO	Dissolved oxygen
EC	Electrical conductivity
GC	Gas chromatography
GHG	Greenhouse gases
IC	Inorganic carbon
N	Nitrogen
N_2O	Nitrous oxide
$NPOC$	Non-purgeable organic carbon
H_0	Null hypothesis
OW	Open water/Lake
P	Phosphorus
KH_2PO_4	Potassium dihydrogen phosphate
KNO_3	Potassium nitrate
RB	Reed belt
$NaHCO_3$	Sodium bicarbonate (soda)
Na_2CO_3	Sodium carbonate
SD	Standard deviation
$T°$	Temperature
TN	Total nitrogen
VCl_3	Vanadium (III) chloride

Chapter 1

Introduction

1.1 Motivation

Natural greenhouse gas (GHG) emissions are as relevant to understand and quantify as anthropogenic ones. The interaction between gases and the hydrosphere is particularly important to consider within the global carbon cycle. It has been estimated that just natural lakes contribute to up to 70% of all freshwater CH_4 emissions (Sanches *et al.*, 2019). Such emissions vary widely depending on the water body's characteristics such as lake age, depth, area, volume and residence time (Soja *et al.*, 2014), making it very hard to precisely estimate global emissions.

Methane (CH_4) is a strong GHG and its emissions from aquatic systems can be significant. CH_4 production takes place mostly in anoxic sediments and it should occur only after sulfate is depleted (Lovley & Phillips, 1987). Once produced, the gas stays in the sediments due to the hydrostatic pressure caused by the water column on top of it and also because CH_4 is barely soluble in water (Torres-Alvarado *et al.*, 2005). Potentially, CH_4 could be released through four different pathways: diffusion, ebullitive flux or ebullition, plant-mediated flux and storage flux, being the latter more common in stratified lakes or when the surface layer freezes (Sanches *et al.*, 2019). Ebullition is one of the less estimated pathways (Sanches *et al.*, 2019), mainly because of its irregular and heterogeneous occurrence.

CH_4 emissions will depend on the difference between its production and its consumption, thus, it is essential to understand the activity of microbial population. There is a variety of methanogenic bacteria that produce CH_4 during the last step of organic matter's anaerobic degradation when the substrate is available (Segers, 1998). They belong to the Archaea domain and represent about 50 species (Torres-Alvarado *et al.*, 2005). Nevertheless, methanotrophs could consume this CH_4 during aerobic or anaerobic CH_4 oxidation. CH_4 oxidizing bacteria and nitrifying bacteria use up CH_4 for their aerobic respiration, which could take place either in the oxic top layer or in the oxic rhizosphere (Segers, 1998). CH_4 anaerobic respiration is particularly important in brackish waters, where CH_4 produced in the deeper layers is transported upwards to the transition zone between sulfate reduction and methanogenesis (Torres-Alvarado *et al.*, 2005).

Local monitoring and site-specific CH_4 estimations are needed to better understand the interaction between carbon, nutrients, microbiological activity, climate and CH_4 emissions (Soja *et al.*, 2014). This study aims to quantify CH_4 emissions in a local Austrian case which has

not yet been intensively studied in terms of its GHG emission potential, focusing mostly on achieving a reliable CH_4 ebullition estimation.

Among the most important ecosystem controls of CH_4 emissions in lakes and wetlands are oxygen conditions, methanogens substrate, organic matter availability and type, plant community composition, water depth, temperature ($T°$) and nutrients concentration (Gholikandi & Sadabad, 2014; Whalen, 2005), which can potentially influence CH_4 formation but also CH_4 consumption. Plants play a special role, providing surface for colonization by CH_4 oxidizing bacteria and organic material for methanogenesis (Torres-Alvarado *et al.*, 2005). Plant phenological stage, activity and composition changes across the year and from plant to plant, affecting directly CH_4 biochemical reactions. Moreover, plants might contribute significantly to CH_4 transport from the sediments up to the atmosphere.

An interesting study was made by Davidson *et al.* (2018) in experimental shallow lakes, describing the impact of $T°$ and nutrients (Nitrogen (N) and Phosphorus (P)) on CH_4 emissions. The results indicated a very strong influence, especially for the ebullition pathway, but also a synergy between these two parameters. Even though this is an experimental study, it serves as an encouraging basis to further study the impact of water quality parameters on CH_4 emissions on the field, which is a much complex environment.

On one hand, according to Magyar *et al.* (2013), Lake Neusiedl presents spatial and temporal heterogeneity with respect to water quality parameters. Open water, reed belt and the anthropogenic influenced zones are some of the main differentiated areas found within the lake regarding water quality. On the other hand, there have been some studies about GHG emissions in Lake Neusiedl, as the one carried out by Soja *et al.* (2014) where ebullition emissions have just been indirectly estimated. These two studies are particularly relevant for the present project which aims to provide a better estimation of ebullition in the lake as well as to find a potential relationship with water quality parameters.

1.2 Research questions

The study is based in the following research questions:

1. **Do nutrients and carbon content in water influence CH_4 ebullition in Lake Neusiedl?**

   The background indicates that nitrate, phosphate and ammonium (studied nutrients) could contribute to CH_4 emissions either by inhibiting CH_4 oxidation or by increasing CH_4 production. At the same time, it is expected that nitrate, its denitrification products (Klüber & Conrad, 1998) and sulphate inhibit CH_4 emissions, mainly because denitrifying bacteria and sulphate-reducing bacteria compete with methanogenic-bacteria for the same substrate (Watson & Nedwell, 1998). It is expected that the former mechanisms are greater than the latter (Davidson *et al.*, 2018; West *et al.*, 2016). Dissolved organic carbon (DOC) has been proved to be an important driving factor for total and diffusive CH_4 emissions (Sanches *et al.*, 2019) so a positive relation between carbon content and CH_4 ebullition emissions is expected.

   H_0: Nutrients and carbon content in water positively relate to CH_4 ebullition.

2. **Does water $T°$ influence CH_4 ebullition in Lake Neusiedl?**

   Water **T°** increases productivity and thus, sediment methanogenesis rates, enhancing CH_4 ebullition (Davidson *et al.*, 2018; West *et al.*, 2016).

   H_0: **T°** contributes positively to CH_4 ebullition.

3. **Are CH_4 ebullition emissions different over space and time in Lake Neusiedl?**

   In different areas of the lake and during a 15-weeks period, it is expected to have differences in CH_4 ebullition emissions due to the spatial and temporal differences on water quality parameters (including $T°$).

   H_0: Methane ebullition emissions are heterogeneously distributed over space and time in Lake Neusiedl.

1.3 Objectives

1.3.1 General

Quantify CH_4 ebullition emissions empirically in Lake Neusiedl and study its potential relationship with water quality parameters.

1.3.2 Specific

- Quantify CH_4 ebullition emissions considering temporal and spatial variability.
- Monitor water quality parameters considering temporal and spatial variability.
- Study statistically the correlation between CH_4 ebullition emissions and water quality parameters.
- Contribute to the understanding of the carbon cycle at an ecosystem scale in Lake Neusiedl.

1.4 Structure of the Thesis

This report is organized into six chapters. The second chapter corresponds to the state of knowledge which pretends to contextualize the topic, summarize the achieved progresses in the field of research and to show potential gaps of knowledge that this study could contribute to fill. It starts by giving an overall picture of the methanogenesis and CH_4 emission processes but then it narrows down to expose what is currently known about water quality parameters as potential drivers of GHG emissions, particularly, CH_4 ebullition emissions. Finally, details of the study site are provided.

The third chapter describes the project itself with specifics on the methodology, materials and instruments used in the field, in the laboratory and for data processing and analysis. Every section is separated into two categories: water and gas.

The fourth chapter presents final results, describing how they were obtained and discussing the most relevant aspects. In-situ parameters, nutrients, carbon content and GHG emissions

outcomes are plotted and summarized in tables. First, each parameter is shown and analyzed independently and then correlations are evaluated statistically.

Finally, the fifth chapter wraps up the report. The main results are summarized and some suggestions are posed in order to be considered in further studies including the perspective acquired throughout this investigation.

Chapter 2

State of Knowledge

2.1 Methanogenesis

CH_4 production, or methanogenesis, is a microbiological process controlled mainly by anoxic conditions and substrate availability (Segers, 1998). Diverse bacteria and archaea biochemically degrade complex organic molecules such as polysaccharides, lipids, and proteins in multiple reactions resulting in CH_4 production (Gholikandi & Sadabad, 2014). The main methanogenic subtrate groups are H_2/CO_2, formate and carbon monoxide, methanol and methyl compounds, and acetate (Gholikandi & Sadabad, 2014). By way of examples, some of the potential chemical reactions are shown below (Torres-Alvarado *et al.*, 2005):

$$CH_3COOH \longrightarrow CO_2 + CH_4 \tag{2.1}$$

$$CO_2 + 4H_2 \longrightarrow CH_4 + 2H_2O \tag{2.2}$$

$$4CH_3OH \longrightarrow 3CH_4 + CO_2 + 2H_2O \tag{2.3}$$

$$4CH_3NH_3 + 2H_2O \longrightarrow 3CH_4 + CO_2 + 4NH_4{}^+ \tag{2.4}$$

Commonly, wetlands sediments can be distinguished by an anaerobic layer where CH_4 is produced by methanogens, and a surficial aerobic layer where CH_4 is oxidized by methanotrophs (Whalen, 2005). The rate of this production/consumption reactions is basically what determines the quantity of CH_4 emitted to the atmosphere, and it depends greatly on lake conditions such as redox potential, $T°$, electron acceptor (or substrate) availability and mixing capacity (Soja *et al.*, 2014). Soja *et al.* (2014) indicates that just about 30 % of CH_4 production reaches the surface annually.

2.2 CH_4 emissions

Wuebbles & Hayhoe (2002) have estimated that natural and anthropogenic sources emit 410-660 $Tg\ CH_4\ y^{-1}$ in total, from which wetlands contribute with 92-232 $Tg\ CH_4\ y^{-1}$ (72 % of natural sources). Bastviken *et al.* (2004) estimated that 8-48 $Tg\ CH_4\ y^{-1}$ correspond to emissions from lakes (6-16 % of natural sources). The radiative forcing of CH_4 is approximately

20-folds higher that the one of carbon dioxide, therefore, a small increase in CH_4 emissions could bring greater impact to climate change (Tranvik *et al.*, 2009)

CH_4 emissions from wetlands are part of an ecosystem process which involves local climatic factors and soil characteristics that influence plant growth, organic matter decomposition, methanogenesis and CH_4 oxidation (Cao *et al.*, 1998). As previously mentioned, CH_4 generated in the anoxic sediments of water bodies can reach the atmosphere througout four pathways:

1. **Diffusion:** CH_4 molecules move driven by a concentration gradient.
2. **Ebullition:** CH_4 bubbles formed in the sediments' interstitial water grow until they can overcome the hydrostatic and atmospheric pressure above it to escape (Torres-Alvarado *et al.*, 2005).
3. **Plant-mediated flux:** includes CH_4 diffusion along the roots, liquid-gas transformation of CH_4 in the root cortex, diffusion through the cortex and aerenchyma and release through micropores and stomata. This transport system is a special aquatic plants' feature evolved as an adaptation to survive anoxic conditions, it basically supplies oxygen to the roots and releases CH_4 to the atmosphere (Torres-Alvarado *et al.*, 2005).
4. **Storage flux:** CH_4 that has been accumulated and stored within the anoxic sediment layer or in the water column because of stratification or ice formation, is suddenly emitted to the atmosphere by diffusion (Sanches *et al.*, 2019).

The ebullition pathway may contribute the most in surface waters, specially in shallow lakes, which is the case in most of the lakes in the world (Sanches *et al.*, 2019). It is a frequent process when lakes are shallower than six meters and methanogenesis rates are high (West *et al.*, 2016). Ebullition emissions are particulary difficult to estimate because of the high uncertainty of the episodic releases, which can be triggered by water table fluctuations or pressure changes (Burke *et al.*, 2019).

2.3 Water quality parameters as GHG drivers

In the literature, some discussion about potential influence of water quality conditions on GHG emissions is ongoing. Site-specific conditions are diverse and the interaction between parameters is complex, thus, this background knowledge should be used just as a reference to understand which parameters would be worth measuring and which correlations should be expected.

Davidson *et al.* (2018) have stated that temperature enhances both CH_4 diffusive and ebullitive fluxes and that nutrients concentration interacts significantly with ebullition emissions. They consider this to be a relevant matter because temperature and nutrients are associated with two of the most relevant issues in freshwater ecosystems: climate change and eutrophication. DelSontro *et al.* (2016) have identified that the relation between temperature and both CH_4 diffusion and ebullition are modulated by the trophic status of the lake, being P the relevant factor. They believe that, for example, low P concentration and low organic substrate availability might diminish temperature influence in CH_4 emissions.

Davidson *et al.* (2015) have found that the effect of temperature is indirectly related to GHG emissions and that main controllers such as nutrients availability and primary producers abundance are indirectly related to temperature. Soja *et al.* (2014) have also found that emergent macrophytes are one of the main drivers of CH_4 emissions while West *et al.* (2016) have established that there is a strong relashionship between lake productivity, methanogenesis and water depth.

Regarding to other factors, Sanches *et al.* (2019) have stated that phosphorous, air temperature, precipitation and dissolved organic carbon were found possitevely related to diffusive flux.

2.4 Case study: Lake Neusiedl

Lake Neusiedl is the western-most and largest steppe lake in Eurasia (Dinka *et al.*, 2010). It is located in the border between Austria and Hungary, approximately 240 km^2 (75 %) belong to Austria and 80 km^2 (25 %) to Hungary (Schranz, 2016). The lake, considered to be a wetland (Magyar *et al.*, 2013), has been part of several studies because of its uniques features. It is very shallow (mean depth of 1.1 m) and 54 % of its surface is covered by *Phragmites australis* (common reed) (Dinka *et al.*, 2010). This vegetated area is referred to as the reed belt.

Phragmites is highly competitive and can grow in diverse soil types under different conditions because it adapts easily to different textures, pH and salinity (Dinka *et al.*, 2010; Schranz, 2016). The reed belt in lake Neusiedl plays an important role not only due to its ecosystem services such as soil erotion protection, water quality enhancer and distinct habitat for several and unique species, but also economically (Magyar *et al.*, 2013). Harvesting the reed once a year brings economic income and contributes with the removal of nutrients that controls its organic succession (Magyar *et al.*, 2013).

Regarding the hydrological balance of the lake, the main water inputs are precipitation (80 %, with a mean of less than 600 mm per year) and, in a much lower extend (20 %), Wulka, Golser Kanal and Rákos patak tributaries (Schranz, 2016). It is dewatered mainly by evapotranspiration. The shallowness of the lake and its reduced catchment area (app. 1 120 km^2) make it prone to climate change (Soja *et al.*, 2013).

Lake Neusiedl has been classified as a "soda-lake" because of its high salt content, composed primarly by soda ($NaHCO_3$) and sodium carbonate (Na_2CO_3) (Schranz, 2016). Its trophic state is mesotrophic-eutrophic with no vertical stratification because of both its shallowness and the strong winds that characterize the region (Schranz, 2016). Turbidity is high because of the same reason, specially in the open water region, discouraging aquatic plants and phytoplankton growth because of the poor light conditions in the water column (Schranz, 2016).

Magyar *et al.* (2013) have separated the lake in three main habitats: reed belt, open water and man-made channels. They have also classified the lake in eight groups regarding water quality characteristics, demonstrating its great spatial and temporal heterogeneity in this regard. Thus, it was essential for this project to select representative locations in the site. The first location represents the open water, a few meters away from the East part of the reed belt zone towards the middle of the lake. It is characterized by its lack of vegetation and its strong N-W winds which cause high turbidity. Fine inorganic sediments give a milky greyish colour to the

water. Depth is about 1.5 m. The second location represents a transition area where artificial channels have been built for boat transit purposes. In particular, this part of the cahnnel where the sampling point was located, is right next to the building of the Illmitz Biological Station, therefore, some human disturbances are frequent. The area is quite protected from the wind so water has low turbidity, allowing aquatic plants and algae to grow easily. The water has a yellow tint with depth also around 1.5 m. The third and last location represented the reed zone, right in the middle of the reed area with access by a boardwalk. Water level varied from 20 cm at the beginning of the measurement period to completly dry at the end. The water has low turbidity as well, yellowish colour and many aquatic plants, insects, fish and frogs. All these diverse characteristics, added to the differences in preliminary water quality parameters measurements, confirmed the heterogeneity of the selected locations. Because of this environmental diversity, differences in CH_4 emissions were expected between locations.

Lake Neusiedl is a well-studied site, several investigations and projects have been carried out in order to understand its geology and hydrology, its biogeochemistry, its role as ecological habitat, its productive value, its birds population, how it is affected by climate change, among many other topics. Nevertheless, its role in the carbon cycle is not fully understood and it is a work in progress to which this research aims to contribute.

Chapter 3

Materials and Methods

The project was carried out in the Austrian part of lake Neusiedl, in the vicinities and with the collaboration of the Illmitz Biological Station (47°46'08"N, 16°45'58"E). Three different locations were selected within the site, which were named reed belt (RB), open water/lake (OW) and channel (CH) (See Figure 3.1). The specific locations were selected mainly because of their differences in water quality conditions, which can be observed in Figure 3.3 and Table 3.1, but also because of their good accessibility.

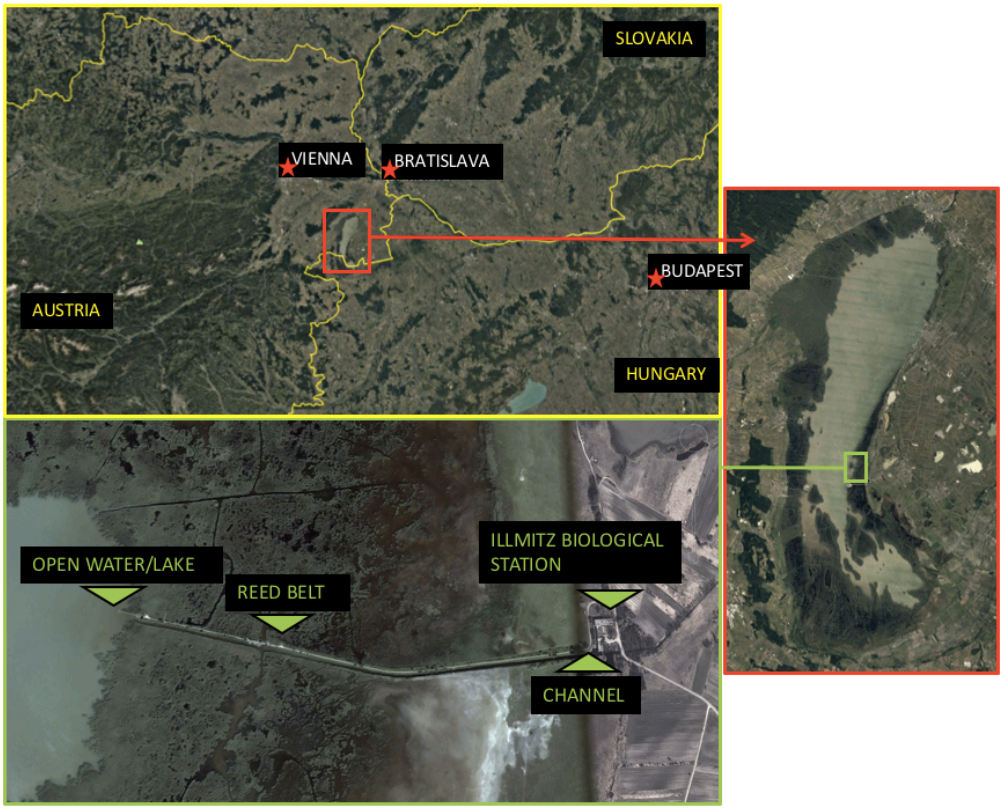

Figure 3.1: Geographic site location and monitoring locations.

On each location ebullition traps were installed permanently for gas collection, which consisted basically in floating body boards with three inverted 23.5 *cm* diameter hdpe funnels pierced through. Each funnel had attached on top a 50 *ml* plastic syringe which was regulated with a three way valve to extract the emerging gases from within (See Figure 3.4). To install the ebullition traps, ambient air was extracted from the funnels and syringes until they

(a) Reed belt location

(b) Open water/Lake location

(c) Channel location

Figure 3.3: Monitoring locations.

were filled with water, so the board could float with the funnels submerged. A HOBO temperature sensor and data logger was fixed to one trap in each location and set to measure every 30 minutes.

Table 3.1: Preliminary measurements of water quality parameters.

Location	**pH**	**T°** $°C$	**DO** $\%$	**EC** mS/cm	**NO_3** mg/L	**NH_4** mg/L	**TN** mg/L	**DOC** mg/L	**Depth** m
Channel	8.45	12.1	91.4	2.71	0.91	0.12	2.51	37.04	1.5
Open water/Lake	8.69	5.7	103.5	1.62	0.82	0.28	1.38	16.26	1.5
Reed belt	8.38	10.7	95.8	2.86	0.15	0.23	2.67	40.14	0.2

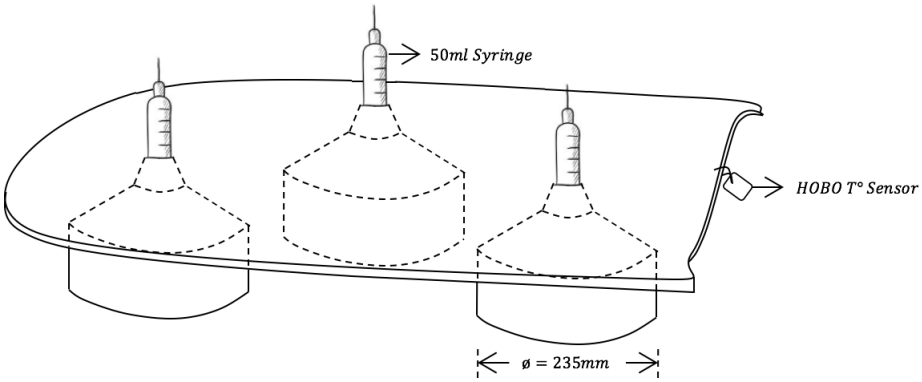

Figure 3.4: Ebullition traps scheme.

Water and gas samples were taken every monitoring day, together with other in-situ measurements described in sections 3.1 and 3.2. From now on, the methodology will be separated in two main stages: field work, where the data and samples were collected, and lab work, where samples were converted into data. Additionally, each of these stages has two separated categories: water and gas. Afterwards, in section 3.3, the methodology used for data processing is explained in detail. Detailed lists of materials, instruments and equipment, and chemicals used on a daily basis on the field and in the lab are shown in Annexes, chapter A.

3.1 Field work

The field work started officially in early spring (30th March 2021, day of the year (DOY) 88) and ended in early summer (14th July 2021, DOY 195). The monitoring frequency ranged between 5-10 days depending on transport and equipment availability. At the beginning and end of the measurement period, 30-31st March and 28-29th June, respectively, day and night measurements were carried out, these days are referred to as campaign days. A total of 16 measuring days were registered for the whole period.

As previously announced, during a field work day, the sampling procedure was separated into two categories which are described in the following two sections:

3.1.1 Water

To monitor the quality of water, in situ parameters were routinely measured at each location and water samples were collected. For the former, a ruler and the water level indicators installed nearby CH and OW locations were used to measure water depth, and a WTW portable multi-parameter analyzer with water $T°$, pH, electrical conductivity (EC), DO and redox sensors was used to measure those parameters. For the latter, water was taken from right next to each trap, filtered, stored in three 20 ml plastic bottles and kept momentarily in a cooling box containing ice packs. Filtration was done first with a MN 619 G $1/4$ $\varnothing 125$ mm filter paper and then, additionally, with a 0.45 μm syringe filter. The samples were afterwards stored at the end of the day in a freezer at -20°C until analysis (Gardolinski *et al.*, 2001; Worsfold *et al.*, 2005).

Additionally, water $T°$ was constantly registered by the HOBO data loggers installed in the ebullition traps at each location and air $T°$ data was downloaded from the Wasserportal Burgenland of the Austrian government website, which has a measurement frequency of 15 minutes.

3.1.2 Gas

To quantify gas emissions, during every sampling date the ebullition traps were checked and gas was extracted when there was more than 1 ml accumulated in the syringes. Extracted gas was injected in 20 ml vacuumed glass vials, sealed with rubber septums and aluminum caps, that were stored in a dry and dark compartment at room $T°$ until analysis.

Additionally, when the equipment was available, in-situ GHG measurements were carried out using a floating chamber connected to a mobile gas analyzer (Los Gatos) during four minutes in order to quantify CH_4 diffusion rates. The chamber was made out of transparent plastic in a 30 cm diameter bird-cage-shape supported in the base with an aluminum plate which was girded with a foam tube as a floating system (see Figure 3.6). During measurements, the chamber was directly connected to the gas analyzer through two 3 mm outer diameter polyurethane tubes, one as inlet and other as outlet, which circulated the air between the closed chamber and the instrument. The GHG concentrations were registered constantly during four minutes, enough time to observe a linear increase because of the accumulation of gases within the chamber.

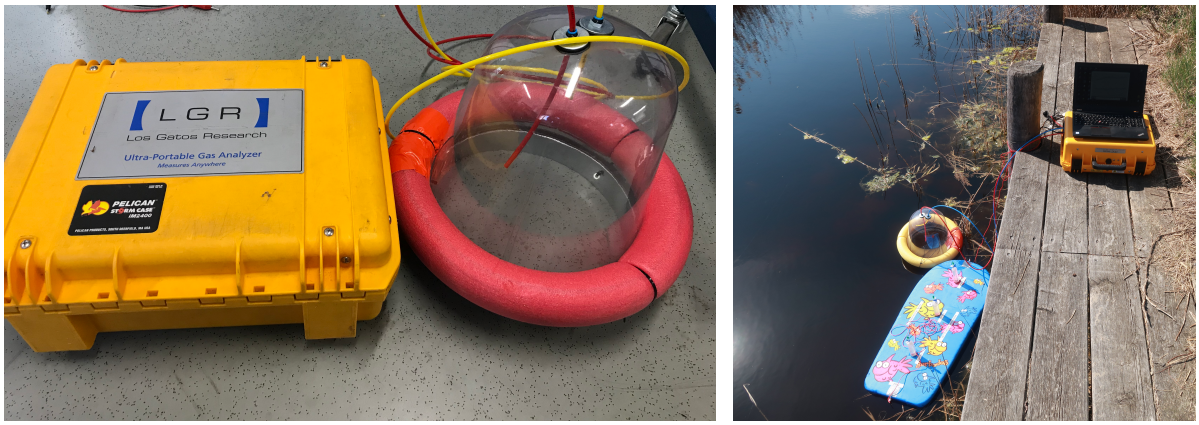

Figure 3.6: Mobile gas analyzer (Los Gatos).

3.2 Lab work

In the Geoecology lab from the University of Vienna, water and gas samples were analyzed separately according to the following two sections:

3.2.1 Water

Three water samples were collected per location next to each of the ebullition traps, and triplicates were made from every one of them. Nitrate (NO_3^-), ammonium (NH_4^+) and orthophosphate (PO_4^{-3}) were determined by colorimetry using a spectrometer (Nano Quant UV-VIS) at 540, 660 and 880 *nm*, respectively. Non-purgeable organic carbon (*NPOC*), inorganic carbon (*IC*) and total nitrogen (*TN*) were determined from the filtered samples by combustion catalytic oxidation using a Shimadzu TOC-L analyzer.

The colorimetric determination protocols were formulated by Dr. Camila Aguetoni Cambui, member of the Geography and Regional Research Institute from the University of Vienna. The procedures used to determine NO_3^- and NH_4^+ are a modification of the methods described by Miranda *et al.* (2001) and Kandeler & Gerber (1988), respectively. The procedure used for PO_4^{-3} determination is based on the method described by Murphy & Riley (1962) and modified for microtiter plates' analysis.

A short description of the final protocols which were used are presented below:

- **Colorimetric determination of NO_3^-**

  1. *Calibration through the preparation of a standard curve:* 1.01 g potassium nitrate (KNO_3) were diluted in 100 ml of high purity deionized water (Milli-Q) to obtain a stock solution of 100 $mmol/L$. 0.5 ml from that solution were once again diluted in 100 ml Milli-Q water to obtain a final concentration of 500 $\mu mol/L$. The standard curve was prepared from this stock solution creating a dilution series ranging from 500 to 1.95 $\mu mol/L$ of KNO_3.
  2. *Microtiter plate preparation:* 75 μl of samples, standards and blanks were pipetted into the plate(s). 75 μl VCl_3 reagent (400 mg vanadium (III) chloride diluted in 50 ml of 1 M hydrochloric acid) were added to reduce NO_3^- to NO_2^- and then 75 μl Griess reagent were added, which is a solution of combined NEDD reagent (50

mg N-napthylethylenediamine dihydrochloride diluted in 250 *ml* Milli-Q water) and sulfanilic acid (1 *g* sulfanilamide diluted in 100 *ml* of 3 *M* hydrochloric acid) in a 1:1 ratio.

3. *Plate(s) incubation:* at 37°*C* for 60 minutes.
4. *absorbance measurement:* at 540 *nm*.

- **Colorimetric determination of NH_4^+**

1. *Calibration through the preparation of a standard curve:* 0.535 *g* ammonium chloride (NH_4Cl) were diluted in 100 *ml* Milli-Q water to obtain a stock solution of 100 $mmol/L$. 0.5 *ml* from that solution were once again diluted in 100 *ml* Milli-Q water to obtain a final concentration of 500 $\mu mol/L$. The standard curve was prepared from this stock solution creating a dilution series ranging from 500 to 1.95 $\mu mol/L$ of NH_4Cl.
2. *Microtiter plate preparation:* 100 μl of samples, standards and blanks were pipetted into the plate(s). 50 μl colour reagent were added, which is a solution of combined 0.3 *M* sodium hydroxide solution, sodium salicylate solution (8.5 *g* sodium salicylate and 63.9 *mg* sodium nitroprusside dihydrate diluted in 50 *ml* Milli-Q water) and Milli-Q water in a 1:1:1 ratio. Finally, 20 μl oxidation solution (0.1 *g* of dichloroisocyanuric acid sodium salt dihydrate diluted in 100 ml Milli-Q water) were added.
3. *Plates incubation:* at room $T°$ (21°*C* app.) for 30 minutes.
4. *absorbance measurement:* at 660 *nm*.

- **Colorimetric determination of PO_4^{-3}**

1. *Calibration through the preparation of a standard curve:* 0.340 *g* potassium dihydrogen phosphate (KH_2PO_4) were diluted in 100 *ml* Milli-Q water to obtain a stock solution of 25 $mmol/L$. 40 μL from that solution were diluted in 10 *ml* Milli-Q water to obtain a final concentration of 100 $\mu mol/L$. The standard curve was prepared from this stock solution creating a dilution series ranging from 100 to 0.39 $\mu mol/L$ of KH_2PO_4.
2. *Microtiter plate preparation:* 200 μl of samples, standards and blanks were pipetted into the plate(s). 20 μl mix solution were added, which is a combination of other three solutions diluted in 100 *ml* Milli-Q water (1.26 *g* ammonium heptamolybdate tetrahydrate diluted in 50 *mL* hot Milli-Q water, 14 *mL* sulfuric acid and 50 *mg* potassium antimony (III) oxide tartrate diluted in 20 *ml* hot water). Finally, 25 μl ascorbic acid solution (44 *mg* ascorbic acid diluted in 10 *ml* Milli-Q water) were added.
3. *Plates incubation:* at room $T°$ (21°*C* app.) for 15 minutes.
4. *absorbance measurement:* at 880 *nm*.

3.2.2 Gas

From ebullition traps' gas samples , CH_4 and carbon dioxide (CO_2) concentrations were determined with a Picarro G2201-i analyzer. For comparison, most of the samples (318 from a total of 417) were measured also with a gas chromatography (GC) system. N_2O concentration

was measured as well with the GC from those samples.

Concentrations were originally unknown, therefore, tests were carried out to determine proper dilution rates for each location (trial phase). Dilution was necessary because in some cases concentrations exceeded the instrument's threshold values and in others to have sufficient volume of sampled gas for making duplicates of each sample with each instrument, but only when the concentration was high enough to do so. The Picarro analyzer used a minimum of 15 *ml* per measurement and for the GC system 40 *ml* were used. The measuring protocol was separated into two groups, samples taken in the RB location and samples taken in the OW and CH locations. The first group was divided into two categories and the second group into three. This is described in detail below:

- For samples taken in the RB location (total RB samples = 161):
  - **When volume collected was $\geq$ 12 ml**: 1 *ml* was extracted from the glass vial and added into a gas bag together with 500 *ml* of N_2. In 10 exceptional cases out of 84 corresponding to this category, different amounts of N_2 were added because they were part of the trial phase in which the best dilution rate was determined.
  - **When volume collected was $<$ 12 ml**: 20 *ml* of N_2 were added into the glass vial first, because the vials were vacuumed before sampling so they required some overpressure to allow the gas being extracted from it. Then, 1, 3 or 5 *ml* were extracted from the diluted gas inside the vial and added into a gas bag together with 300, 200 and 150 *ml* of N_2, respectively. In 14 exceptional cases out of 77 corresponding to this category, different amounts of N_2 were added because they were part of the trial phase.
- For samples taken in the OW and CH locations (total OW samples = 110, total CH samples = 134):
  - **When volume collected was $\geq$ 39 ml before DOY 142**: The first set of measurements (40 samples) was done without dilution because the gas bags were not available yet, so only samples with at least 30 *ml* easy to extract were previously measured in duplicates with the Picarro. RB samples had too high concentrations to be measured without dilution, so this case applies just for samples taken in the OW and CH locations. These samples were measured once again later on using the GC, extracting 5 *ml* of sample directly from the glass vial and added into a gas bag together with 100 *ml* of N_2.
  - **When volume collected was $\geq$ 13 ml**: 3 or 5 *ml* of sample were extracted from the glass vial and added into a gas bag together with 120 ml of N_2. For 10 samples, 5 *ml* of sample were extracted and diluted in 250 *ml* of N_2 so in this case triplicates could be done with both instruments. In 8 exceptional cases out of 95 corresponding to this category, different amounts of N_2 were added because they were part of the trial phase.
  - **When volume collected was $<$ 13 ml**: 15 *ml* of N_2 were added to the glass vial first and then 5 *ml* were extracted from the diluted gas inside the vial and added into a gas bag together with *ml* of N_2. In this case, the volume was not enough to measure with the GC so triplicates were measured with the Picarro instead. Further diluting of the samples in order to increase their volume resulted risky because the concentrations were already too close to the minimum guaranteed range from the

equipment of 1.8 ppm of CH_4. For 10 samples, 150 ml of N_2 were added in order to measure at least some of this category with the GC. These were selected among the locations with higher concentration in the previous measurements. In 6 exceptional cases out of 99 corresponding to this category, different amounts of N_2 were added because they were part of the trial phase.

Ideally, the same methodology should have been applied to each case, but the difficulty of predicting the range of concentration in space and time did not make it possible.

3.3 Data processing and statistical analysis

The main software used for data processing and statistical analysis was R 4.0.3. The procedures used in every stage are shortly explained below:

3.3.1 Water

Water samples were analyzed with spectrophotometry, therefore, results were given as absorbance values (%). absorbance was then transformed to concentration units using a standard curve to create a linear regression. The intercept was fixed to the average of the blanks. The R^2 was always higher than 0.98.

Analysis of variance (one way ANOVA) and Tukey-HSD tests with level of significance of 5 % ($\alpha = 0.05$) were carried out in order to evaluate statistically significant differences between sampling locations. Shapiro-Wilk and Levene's tests were used to confirm that the assumptions of normality and homoscedasticity of the data were met.

3.3.2 Gas

For ebullition measurements the data was obtained directly in concentration units (ppm) but it had to be transformed to consider the dilution rates used in each case (described in detail in subsection 3.2.2). To transform these concentration values into fluxes, they were first transformed to mass per unit volume according to Boguski (2006) and then time of collection and area of the funnel were considered. The equation used to estimate GHG ebullition fluxes was the following:

$$F_{Eb-GHG} = \frac{[GHG]_{ppm} V_{occ}}{A_{fun} \Delta t} * m \tag{3.1}$$

Where F_{Eb-GHG} is the ebullition flux of gas in $\mu g m^{-2} d^{-}1$ and $[GHG]_{ppm}$ is the gas concentration in ppm given by the Picarro instrument. V_{occ} corresponds to the total volume of occurred gas in the respective syringe from where the gas was collected, in litres. A_{fun} is the funnel area (0.0434 m^2) and Δt is the elapsed time in days. m is a transformation factor which depends on the kind of GHG (0.656 for CH_4 and 1.8 for CO_2 and N_2O).

The ebullition flux was also calculated in $mg m^{-2} h^{-}1$, in which case equation 3.1 was divided by 10^3 and Δt was transformed to hours. To estimate the mean ebullition emission rate at each location for the entire period ($F_{Eb-GHG}*$), equation 3.1 was modified into equation 3.2,

where n is the total number of measurements available at each location and Δt considers the entire measurement period.

$$F_{Eb-GHG}* = \frac{\sum m[GHG]_{ppm} V_{occ}}{A_{fun} \Delta t} \tag{3.2}$$

Two-sample t-tests with level of significance of 5 % (α = 0.05) were carried out in order to evaluate statistically significant differences between measurement equipments and between sampling locations. Number of samples ($n > 50$) and Levene's test were used to confirm that the test assumptions were met.

To evaluate correlation between gas and each water quality parameter, they were plotted against each other and a linear regression model was fitted. In few cases, logarithmic and exponential regressions were used because they fitted better. R^2 was analyzed for each case and later comparison was done. The relationship was considered high when $R^2 \geq 0.6$, moderate when $0.4 \geq R^2 < 0.6$ and low when $0.2 \geq R^2 < 0.4$. No relation was determined when $R^2 < 0.2$. In most of the cases, due to highly skewed data, log-transformations were applied (Benoit, 2011).

From diffusion measurements, only the data that fitted a linear regression with $R^2 \geq 0.75$ was used. According to Pihlatie *et al.* (2013), the equation used to estimate GHG diffusion fluxes is the following:

$$F_{Diff-GHG} = \frac{S}{10^6} * \frac{V_c M_m}{V_m A_c} * 3600 \tag{3.3}$$

Where $F_{Diff-GHG}$ is the diffusion flux of gas in $gm^{-2}h^{-}1$, S is the calculated slope of accumulated concentration over time, divided by the factor 10^6 for concentrations in ppm. V_c corresponds to the volume of the chamber (0.0165 m^3), A_c is the chamber area where the gas exchange between air and water occurs (0.0707 m^2). V_m and M_m are molar volume and molar mass, respectively.

Chapter 4

Results and Discussion

The main results obtained from data processing and statistical analysis are presented and discussed in this chapter.

4.1 In-situ parameters

Figure 4.1 shows the rolling daily average of water temperature per location and overall air temperature obtained from the data collected from the HOBO sensors and the Wasserportal Burgenland, respectively. Unfortunately, the OW location had a significant gap of missing data due to the loss of one of the sensors in one of the frequent strong waves events. The fluctuations were significant, specially for air temperature, but there was a clear and steady increase over the measurement period. The mean, minimum and maximum registered temperatures are shown in Table 4.1. In average, the RB location registered the highest water temperatures, followed by the CH and finally the OW.

Figure 4.1: Water mean $T°$ registered at each location for the HOBO sensors and overall mean air $T°$ registered at Illmitz station and downloaded from the Wasserportal Burgenland of the Austrian government website.

Table 4.1: Mean, minimun and maximum air and water $T°$.

T° type	**Mean T°** $°C$	**Min T°** $°C$	**Max T°** $°C$
Air	16.6	-2.0	35.2
Channel water	17.2	2.8	36.3
Open water/Lake water	14.9	2.9	35.0
Reed belt water	19.5	2.8	39.4

The 15-weeks measurement period started in early spring and finished in early summer. During that period, water temperatures ranged between 3 and 37$°C$, evidencing seasonal changes. The new reed started to grow fast as well as aquatic plants and algae. $T°$ and vegetation promoted microbial activity so it was expected to have an increase in CH_4 production and, eventually, in CH_4 ebullition emissions.

Figure 4.3 shows the in-situ parameters registered values. On DOY 88-89 and 179-180 the sets of data were denser because during campaign days these parameters were measured every six hours. For those days, mean values for each location are shown at day and night to be able to observe daily variations. Tables 4.2 and 4.3 summarize the mean, minimum and maximum values for each location.

Table 4.2: In-situ water quality parameters summary: water $T°$, pH and EC.

Location	**Water T°[°C]**			**pH**			**EC[mS/cm]**		
	mean	min	max	mean	min	max	mean	min	max
Channel	20.6	7.8	30.4	8.49	8.24	8.61	3.00	2.70	3.70
Open water/Lake	19.6	6.1	29.4	8.89	8.77	9.01	2.90	2.53	3.19
Reed belt	20.4	8.3	36.0	8.63	8.18	9.03	4.75	3.22	7.87

Table 4.3: In-situ water quality parameters summary: DO, redox potential and water depth.

Location	**DO[%]**			**Redox potential [mV]**			**Water depth [cm]**		
	mean	min	max	mean	min	max	mean	min	max
Channel	68.0	15.3	120.4	121.6	-139.3	242.3	139.3	127.0	150.0
Open water/Lake	96.3	76.7	106.2	124.5	-38.9	206.3	139.1	127.0	150.0
Reed belt	74.2	0.0	192.1	36.9	-300.2	201.1	12.1	0.0	19.5

In this case, $T°$ seems to be more similar in between locations compared to Table 4.1, which might be because these measurements were always taken around the same time of the day (between 09:00-17:00 app.) and did not consider daily fluctuations, except during campaign days.

The highest mean pH was registered in the OW with a value of 8.89 and the lowest in the CH with 8.49. Alkaline conditions are normal in this lake. EC values were evidently different between locations but, overall, values were high due to the high lake salts content. In the RB, EC was always higher than in the CH and OW with a mean of 4.75 mS/cm, while in the CH and OW locations, 3 and 2.9 mS/cm were the mean values, respectively. The shallowness in the RB might be an explanation for this, because evaporation resulted in a severe water level drop

of about 20 *cm*, increasing salts concentration.

Oxygen levels were relatively constant until DOY 132 in all locations, after that, in the CH and RB the *DO* values varied widely from 15.3 to 120.4 % and from 0 to 192.1 %, respectively. This might be due to fluctuations in the water level and an increase in the presence of aquatic plants and algae. It is important to highlight that the measurements were taken 5-10 *cm* below the water table, it would have been interesting to measure it at different levels, including the sediments.

Redox potential showed a steep decrease, reaching negative values in all locations during the last campaign days (DOY 179-180). The RB location was the one with the lowest values, registering a mean of 36.9 mV, while the CH and OW had means of 121.6 and 124.5 mV, respectively. Soil redox potential would have provided important aditional information to the understanding of methanogenesis and where this process was being carried out. Lovley & Phillips (1987) determined that CH_4 production requieres values under -244 mV to occur. During the last days in the RB, when there was still a few centimeters of water, oxygen levels were close to zero and values lower than this threshold were reached. Thus, a peak in CH_4 emissions was expected for this period.

Water depth also decreased steadily after DOY 142, explained by the lack of precipitation and increase in $T°$. RB location dried off at the end of the measurement period, therefore, it was not possible to collect water samples during the last two monitoring days for this location (see Figure 4.2). Water depth is a crucial parameter for wetlands hydrology, in particular for this lake, which had overcome adverse drought events several times in the past. When wetlands dry out, sediments get in direct contact with the atmosphere and large amounts of GHGs could be release and cause large environmental impact.

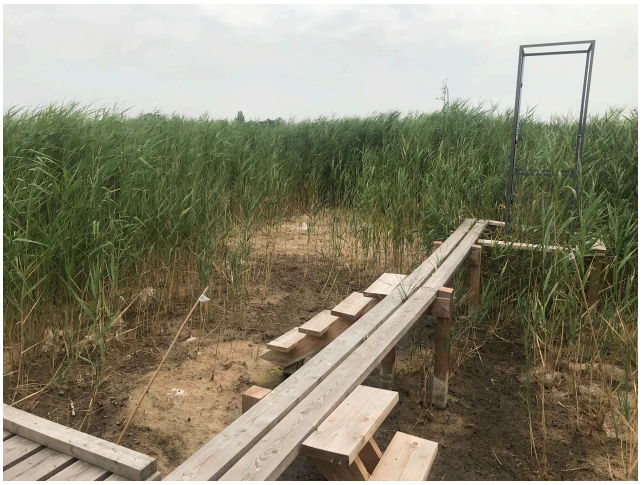

Figure 4.2: RB location DOY 195.

In-situ parameters are always recommended to measure during any water monitoring procedure. Even when they were not the main focus of this study, they were essential to assess every analysis, to understand the context and to relate behaviour between different parameters.

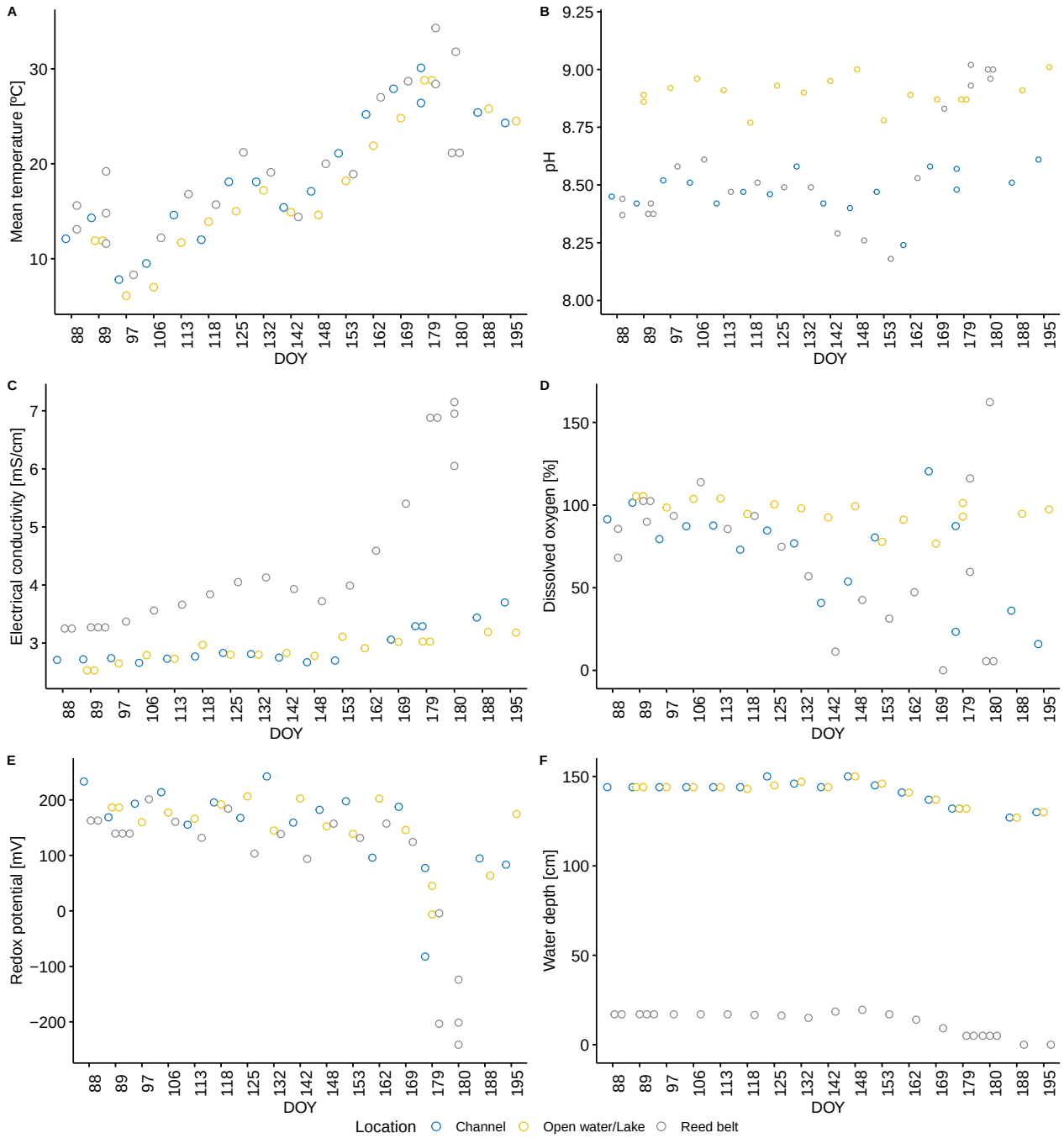

Figure 4.3: In-situ water quality parameters measured at each location. A: Water $T°$, B: pH, C: EC, D: DO, E: redox potential and F: water depth.

4.2 Nutrients

TN, NO_3^-, NH_4^+ and PO_4^{-3} were determined in the lab from water samples collected during monitoring days. Figure 4.4 shows mean concentrations per day and location including their standard deviation (SD) while Tables 4.4 and 4.5 show a summary of all samples measured.

Table 4.4: Nutrients summary: TN, NO_3^- and NH_4^+.

Location	**TN**$[\mathbf{mg/L}]$			**NO$_3^-$**$[\mu\mathbf{g/L}]$			**NH$_4^+$**$[\mu\mathbf{g/L}]$		
	mean	min	max	mean	min	max	mean	min	max
Channel	1.98	1.18	2.90	48.35	0.00	178.17	74.88	0.00	570.00
Open water/Lake	1.38	0.00	4.38	192.40	0.00	718.72	132.71	0.00	978.00
Reed belt	4.28	0.98	7.36	29.34	0.00	183.78	88.09	0.00	442.5

Table 4.5: Nutrients summary: PO_4^{-3}.

Location	**PO$_4^{-3}$**$[\mu\mathbf{g/L}]$		
	mean	min	max
Channel	239.94	46.83	544.25
Open water/Lake	45.35	0.00	254.65
Reed belt	76.73	2.13	584.56

In general, TN values were about two orders of magnitude higher than NO_3^- and NH_4^+, which indicated that there must be important organic N sources. This suggests that, in average, organic N could correspond to up to 77.1, 93.5 and 97.4 % of all N compounds present in the OW, CH and RB waters, respectively. TN in the RB was more than double than in the CH and OW, with mean values of 4.28, 1.98 and 1.38 mg/L, respectively. Thus, OW presented the lowest values of TN but the highest NO_3^- and NH_4^+ concentrations, while the RB presented the highest values of TN but the lowest inorganic N content. Inorganic N sources in Lake Neusiedl are River Wulka (32 %), wet deposition (31 %), dry deposition (25 %), other tributaries (6%) and point sources (5%) (Soja *et al.*, 2014).

PO_4^{-3} showed significant differences in all locations, with an average of 239.94, 76.73 and 45.35 $\mu g/L$ in the CH, RB and OW, respectively. PO_4^{-3} concentration is strongly influenced by the water level because it determines the exchange with the reed belt (Schranz, 2016). This could explain the clear increase in the CH from DOY 148, when also the water depth started to decrease steadily (see Figures 4.3F and 4.4D). Dry periods could mean less accumulation in the reed because there is less surface in contact with water for exchange. In the RB and CH locations a less pronounced peak could be also observed and it could be due to the same reason. Higher levels in DOY 97 and 118 could be explained by the strong winds during the first days of measurement, which could have brought up PO_4^{-3} from the sediments (Schranz, 2016).

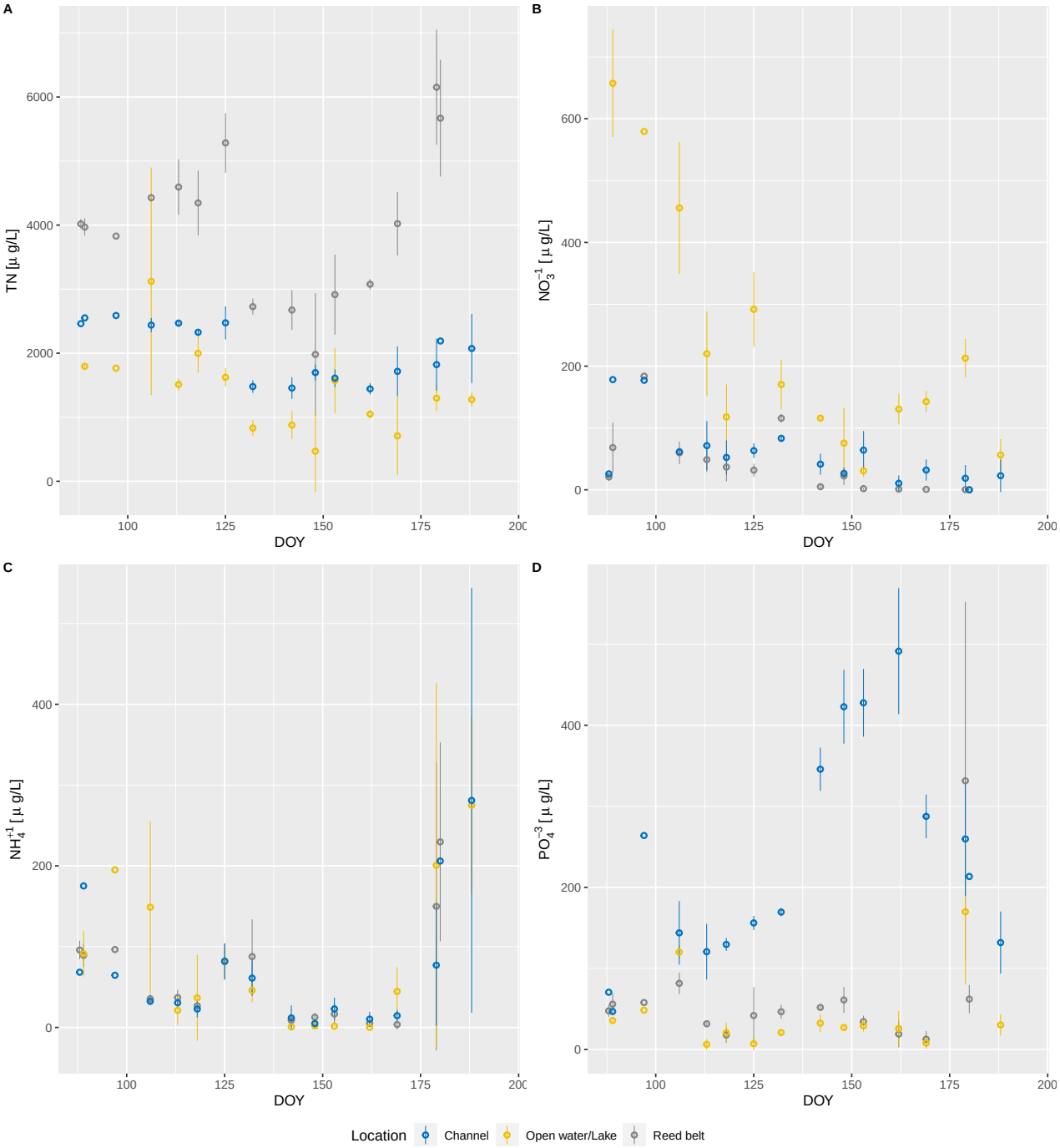

Figure 4.4: Mean nutrients concentrations with their SD per DOY and location. A: TN, B: NO_3^-, C: NH_4^+ and D: PO_4^{-3}.

Analysis of variance (one way ANOVA) and Tukey-HSD tests with level of significance α=0.05 were carried out on nutrients concentrations data to compare whether there were significant differences between the different locations or not, results are summarized in Table 4.6. For all nutrients, except NH_4^+, there were significant differences between some or all locations. The p-values < α for the ANOVA test indicated that there were significant differences between locations and p-values < α for the Tukey-HSD test indicated between which locations in particular did these differences occur. For NH_4^+, the ANOVA test showed that there were no significant differences between locations (p-value=0.164 > α=0.05).

Table 4.6: ANOVA and Tukey-HSD tests results for Nutrients v/s Location.

		p-value Tukey-HSD			
Nutrient	**p-value ANOVA**	**OW/CH**	**RB/CH**	**RB/OW**	**Significant differences**
TN	8.56E-06	0.065539	0.000031	0.000009	Between RB/CH and RB/OW
NO_3^-	8.52E-03	0.016871	0.930328	0.011344	Between OW/CH and RB/OW
NH_4^+	1.64E-01	NA	NA	NA	No
PO_4^{-3}	1.75E-05	0.000016	0.000113	0.014194	Between all locations

4.3 Carbon

NPOC and *IC* were determined in the lab from the water samples collected during monitoring days. Figure 4.5 shows the results of the calculations to get the mean concentration per day and location, including their SD. Table 4.7 shows a summary of all samples measured.

Table 4.7: Carbon summary: *NPOC* and *IC*.

Location	**NPOC[mg/L]**			**IC[mg/L]**		
	mean	min	max	mean	min	max
Channel	43.95	30.66	78.68	253.98	163.6	365.9
Open water/Lake	27.68	18.01	39.05	165.98	93.53	339.50
Reed belt	87.95	52.44	190.60	282.50	111.80	511.60

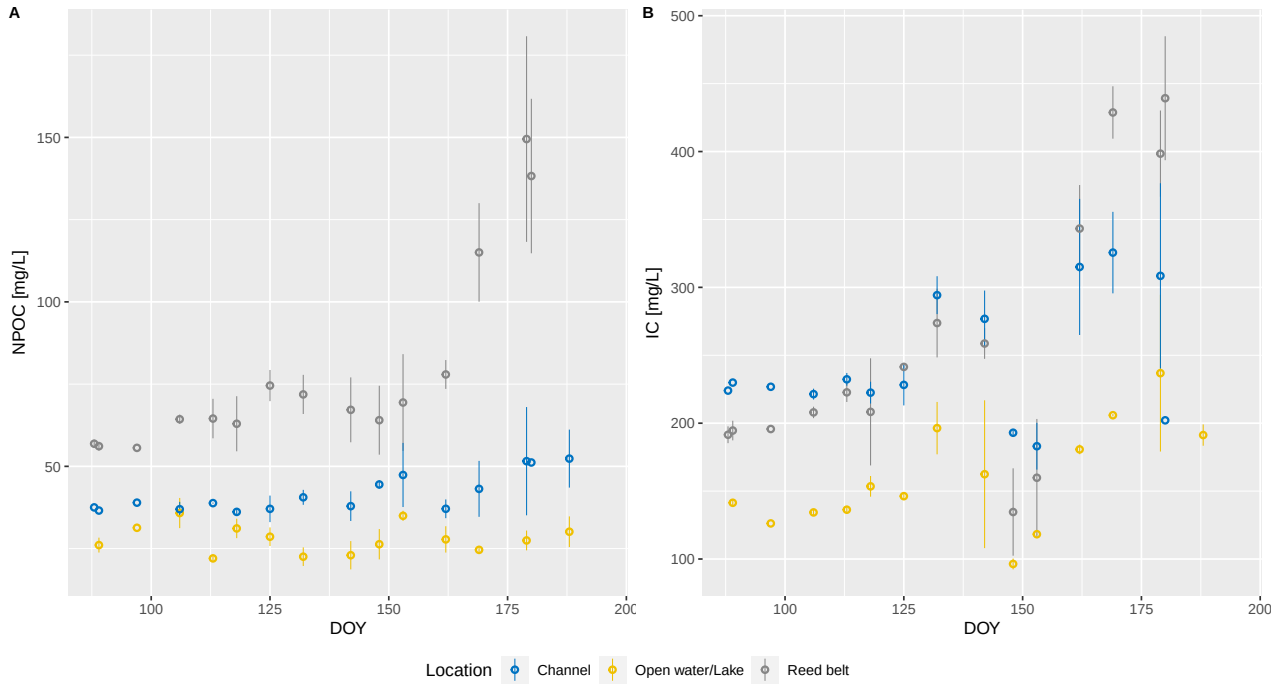

Figure 4.5: Mean carbon concentrations with their SD per DOY and location. A: *NPOC* and B: *IC*.

Inorganic content is very high with respect to the organic, which is usual in water. It includes free CO_2, carbonate ion (CO_3-2) and bicarbonate ion (HCO_3^-). The organic portion corresponded only to 14.3, 14.8 and 23.7 % of the total carbon, in the OW, CH and RB, respectively. This might be explained by the high pH and agricultural activity in the region, characteristics that have been associated with higher total inorganic carbon (Rantakari & Kortelainen, 2008).

Besides, organic matter decomposition could also play a role (Rantakari & Kortelainen, 2008).

Both, *NPOC* and *IC* concentrations, fluctuated in time. Overall trends were to increase or accumulate, except for the organic content in the OW which was always lower and more stable, probably due to a thinner sediment layer in the OW and to a lower content of organic matter available for mineralization there (Soja *et al.*, 2014). The increase in organic carbon in the CH and RB can be associated to an increase in primary production of algae and macrophytes (Rantakari & Kortelainen, 2008).

As with nutrients, one way ANOVA and Tukey-HSD tests (α=0.05) were carried out to compare whether there were significant differences between different locations or not, results are summarized in Table 4.8. From the analysis, it was concluded that in all cases there are significant differences between all locations.

Table 4.8: ANOVA and Tukey-HSD tests results for Carbon v/s Location.

		p-value Tukey-HSD			
Carbon	**p-value ANOVA**	**OW/CH**	**RB/CH**	**RB/OW**	**Significant differences**
NPOC	7.72E-06	0.024571	0.000035	0.000008	Between all the locations
IC	5.11E-05	0.003936	0.001014	0.000041	Between all the locations

4.4 GHG emissions

During this section, different analysis are shown. The main focus of this study was to analyze the relationship between CH_4 ebullition emissions and water quality parameters, which is covered in the first two subsections (4.4.1 and 4.4.2). CH_4 diffusion and CO_2 and N_2O ebullition emissions are covered in the last two subsections (4.4.3 and 4.4.4, respectively).

During monitoring days, the amount of collected gas increased steadily as time passed by and seasons changed. Figure 4.6 illustrates this increment. In the OW location there was a marked increase between DOY 118 and 142, during those days the strong winds and waves might have let some ambient air go inside the ebullition traps but they also might have triggered gas bubbles to come up to the surface. With the reactivation of plants activity and increase in water T°, an immediate increase in CH_4 ebullition is observed in response. This trend was expected to continue further and reach its peak during late summer or beginning of Autumn.

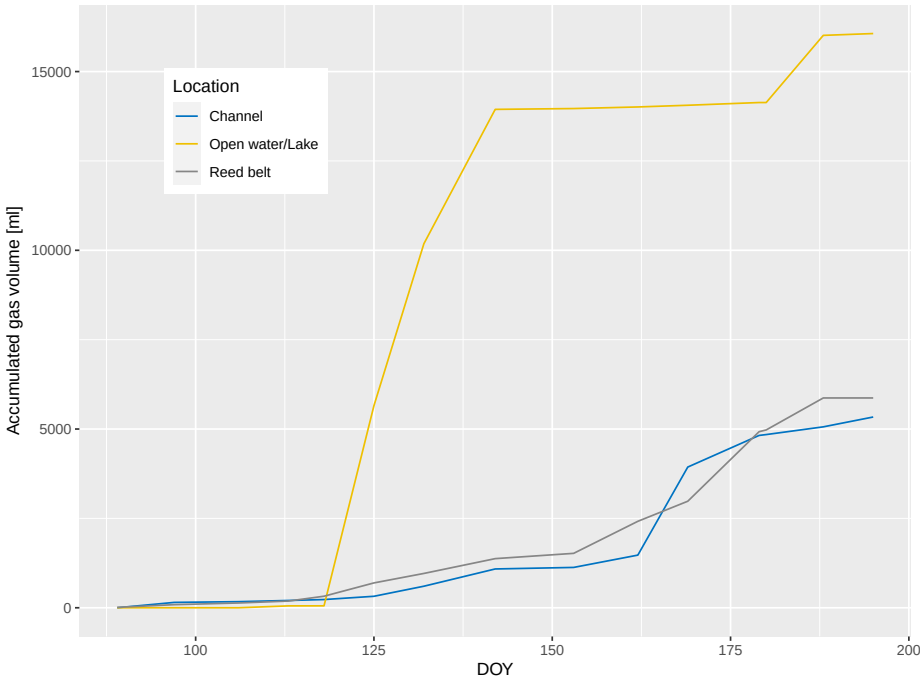

Figure 4.6: Accumulated gas volume collected over time.

4.4.1 CH_4 concentrations and ebullition emissions

Duplicates of the samples were measured with two different instruments: Picarro and GC. Bubbles' CH_4 concentrations (ebullition concentrations) were given diretly in *ppm* (see results in Annexes, chapter B.1). Figure 4.7 shows the values obtained from both instruments plotted against each other and fitted to a linear regression with $R^2 = 0.97$.

Aditionally, a two-sample t-test ($\alpha = 0.05$) was carried out with the CH_4 concentration data of each location in order to compare whether there were significant differences between the two instruments or not, the results are summarized in Table 4.9. In all cases the absolute critical value is greater than the absolute t-value and the p-value is greater than α, therefore, the null hypothesis that states that both measurements are not significantly different cannot be rejected. Because of this, hereafter, just data obtained from Picarro, which is larger, will be used.

Table 4.9: Two-sample t-test results for GC v/s Picarro.

Location	**t-value**	**Degrees of freedom**	**Critical value**	**p-value**
Channel	-0.184	252	1.969	0.854
Open water/Lake	-0.671	242	1.970	0.503
Reed belt	0.906	332	1.967	0.366

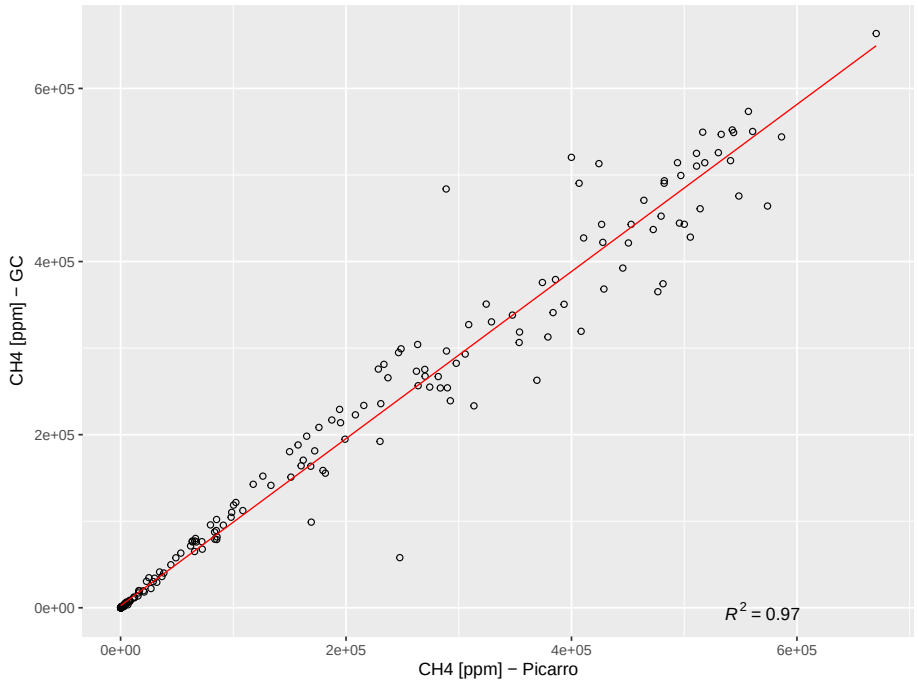

Figure 4.7: CH_4 concentrations for all locations: GC v/s Picarro.

Mean CH_4 ebullition concentrations were 937.9, 1 034.9 and 204 211.5 ppm in the OW, CH and RB, respectively. A two-sample t-test ($\alpha = 0.05$) was carried out between OW and CH to compare whether there were significant differences in CH_4 concentrations between these two locations or not. Results indicated that there were not significant differences (p-value = 0.869). No comparison with RB was done because the values were in average two orders of magnitude higher than in the CH and OW.

As previously mentioned in subsection 3.3.2, CH_4 concentrations were transformed to fluxes using equation 3.1. The results are shown in Figure 4.8, where plot A corresponds to the CH and OW locations, and plot B to the RB. They were presented in two different plots because of the great differences in emission rates. The two-sample t-test carried out with flux values delivered the same conclusions than the one with concentrations, with a p-value = 0.0481. Mean CH_4 ebullition rates were 35.6, 118.4 and 17 053.7 $\mu g\ CH_4\ m^{-2}d^{-1}$ in the OW, CH and RB, respectively. Even though the emission' scales were two orders of magnitud higher in the RB with respect to CH and OW, the trend was similar, with a clear peak in DOY 125 for all locations and a smaller peak in DOY 125 for the OW and RB locations. This was congruent with the T° peaks observed in Figure 4.3.

Mean ebullition emission rates were estimated at each location for the entire period using equation 3.2, obtaining rates of 50.23, 85.13 and 34 064.62 $\mu g\ CH_4\ m^{-2}d^{-1}$ in the OW, CH and RB, respectively.

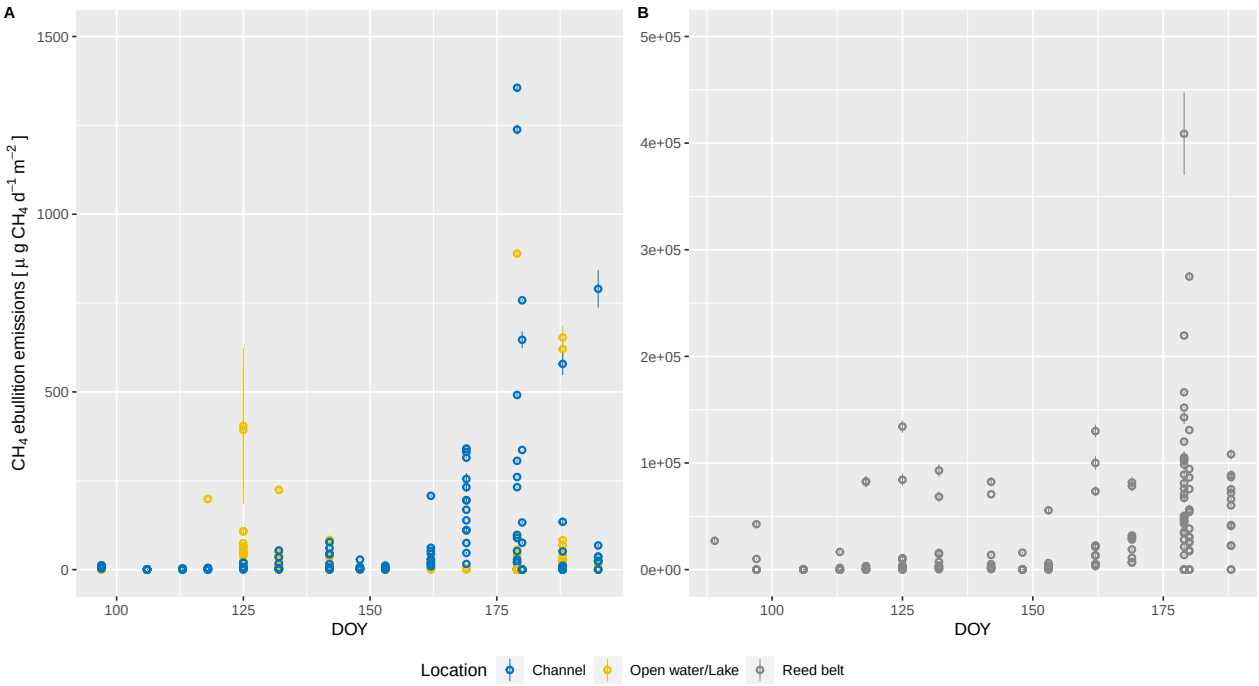

Figure 4.8: CH_4 ebullition emissions with their SD for A: CH and OW, and B:RB.

4.4.2 CH_4 ebullition emissions v/s water quality parameters

In this section, CH_4 ebullition emission rates and water quality parameters were compared using linear regressions between CH_4 ebullition emissions and each measured parameter. In few cases, logarithmic and exponential regressions were used because they fitted better. The degree of significance for R^2 was previously defined in subsection 3.3.2.

First of all, the parameter in question was analyzed as a single factor over the complete data set, which gives information of the overall relation between the parameter and the CH_4 ebullition rate under any condition. Then, even when results of the first analysis were insufficient to conclude any correlation, the parameter was analyzed per location, which means that the variation of the parameter under specific characteristics of each location was assessed. For nutrients and carbon content all graphs are shown but for in-situ parameters only the ones with some correlation are presented.

When all data was analyzed together, TN showed moderate correlation with CH_4 ebullition emissions (R^2 = 0.57) but when the analysis was carried out in every location separately, there was no relation, with R^2 = 0.16, 0.055 and 0.047 for RB, OW and CH, respectively (see Figure 4.9). This could be interpreted as a higher probability of recording higher CH_4 ebullition emissions occurring in locations with higher TN, when TN is considered as the only variable factor. Nevertheless, in a particular location, temporal changes in TN did not seem to have a direct effect in CH_4 ebullition rates.

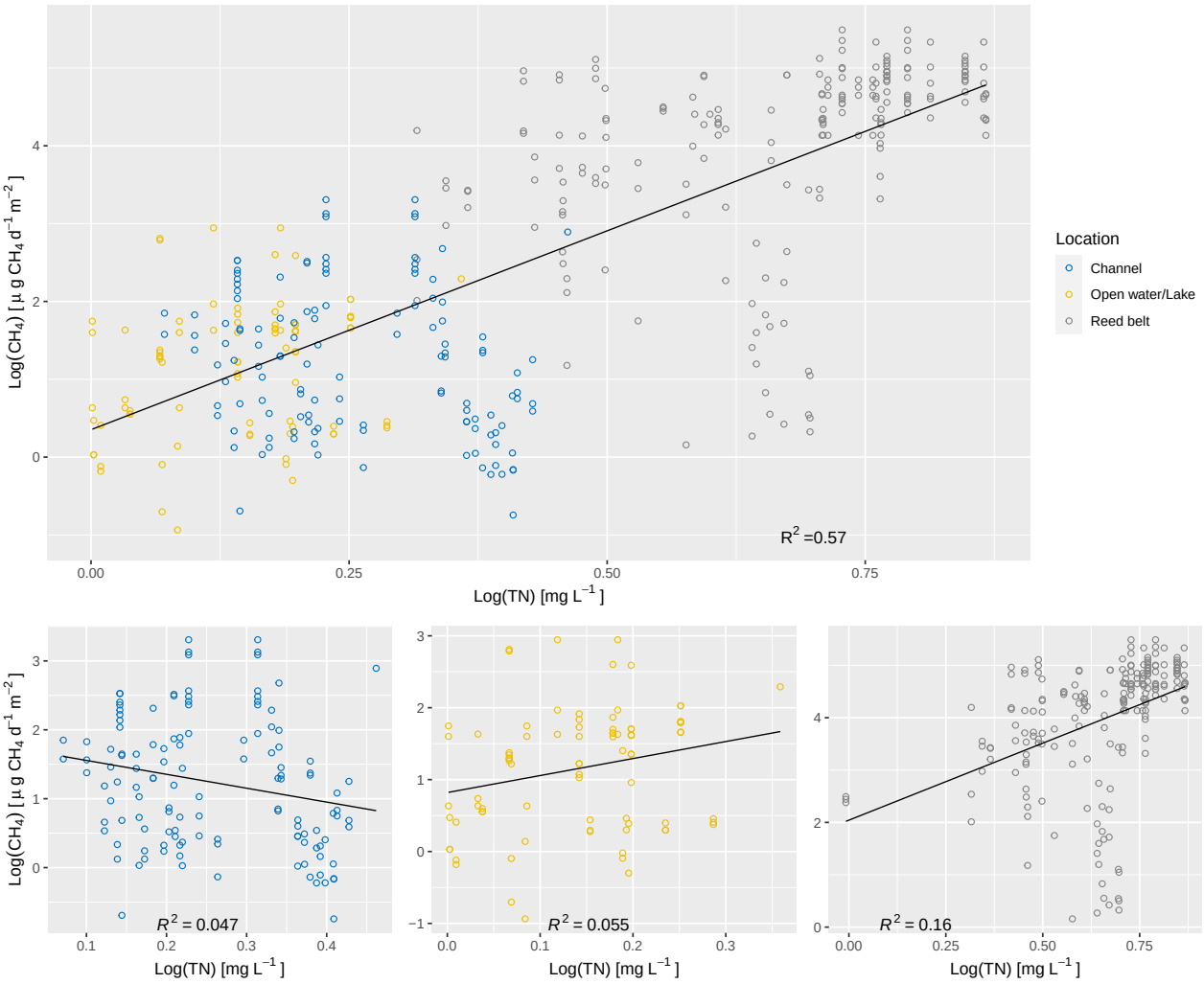

Figure 4.9: Ebullition emissions v/s TN.

Even though TN levels were high are had a high correlation with CH_4 ebullition emissions, it did not indicate relation with N as a nutrient because it had been concluded that the most part of TN would correspond to its organic forms.

NO_3^- represented a small portion of TN, however, the behaviour was different when comparing it to CH_4 ebullition emission rates (see Figure 4.10). No correlation was established in any case, with $R^2 = 0.098$ when comparing the whole data and $R^2 = 0.15$, 0.094 and 0.072 in OW, CH and RB, respectively, when the comparison was made for each location separately. The linear regressions were negative except in the OW. NH_4^+ and PO_4^{-3} were the parameters that showed the lowest correlation with CH_4 ebullition emissions when the complete data set was analyzed, with $R^2 = 0.034$ and 0.0071, respectively. Locally, the correlations were not better.

In conclusion, nutrients did not show any relevant correlation with CH_4 ebullition emissions. The effect of NO_3^- and NH_4^+ might be negligible because their concentrations are low, indicating that there is a limitation of N in its inorganic form, which is the one that plants and other microorganisms consume, for example, methanotrophs. P concentration has been associated with diffusion emissions rather than with ebullition emissions (Sanches *et al.*, 2019).

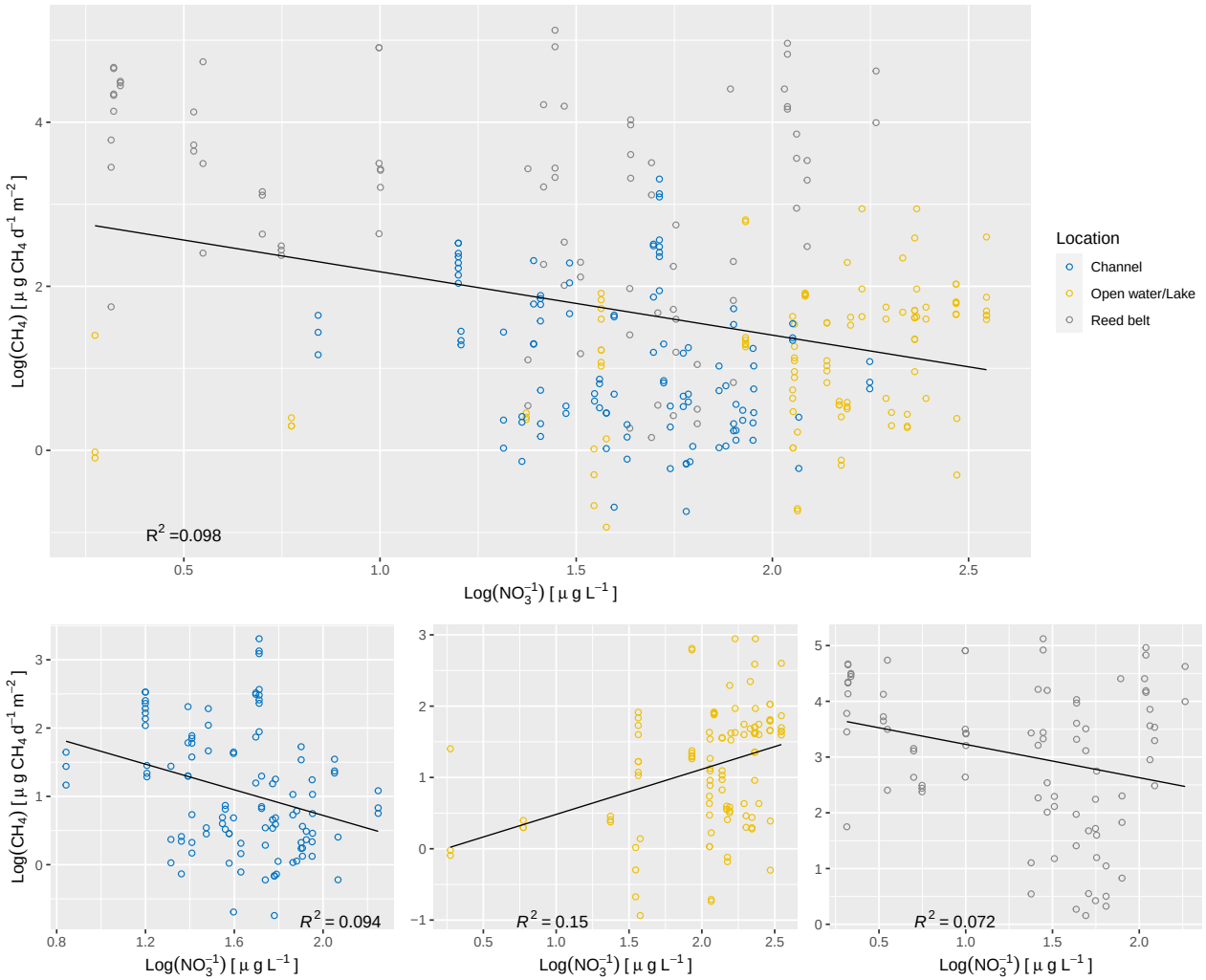

Figure 4.10: Ebullition emissions v/s NO_3.

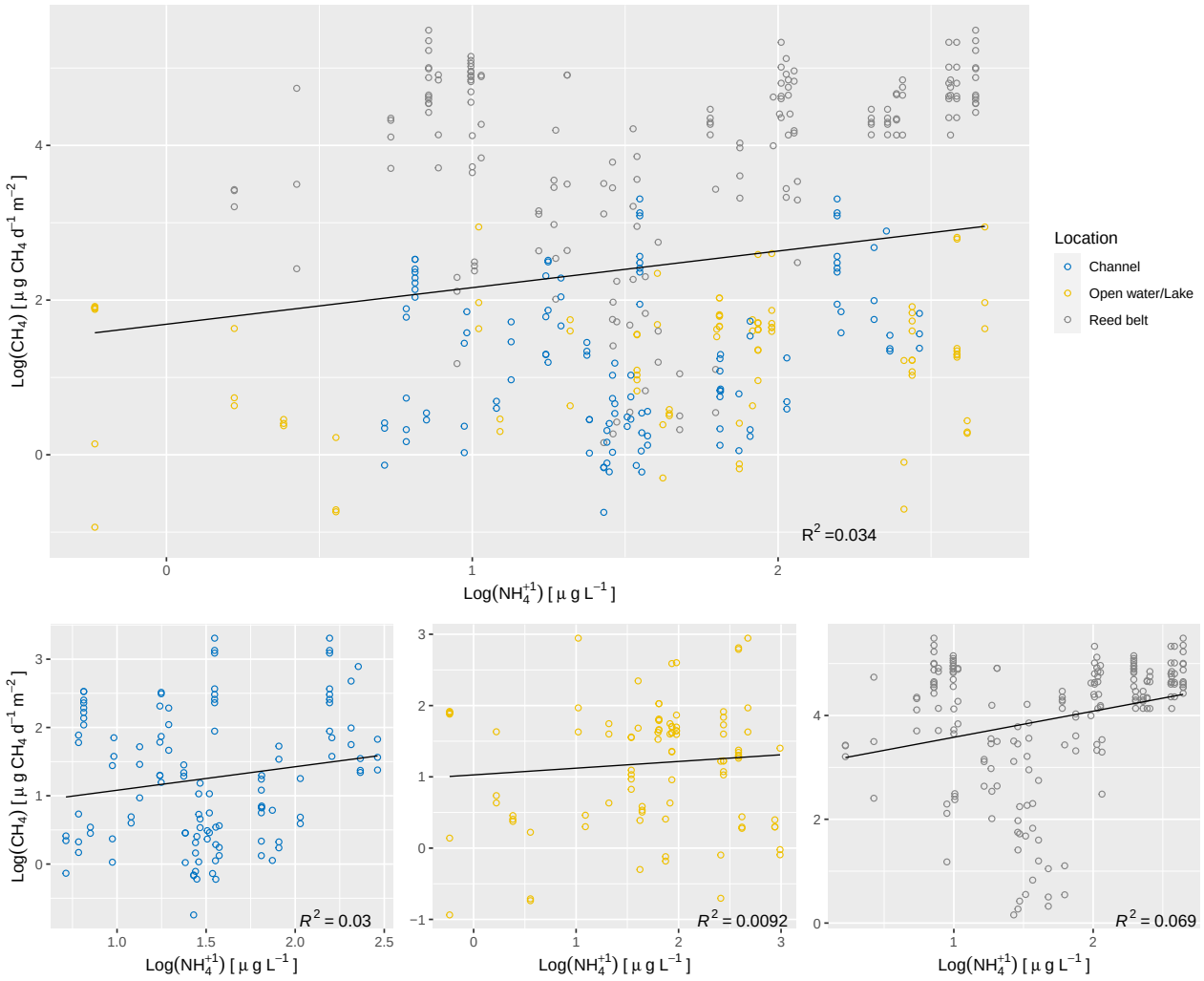

Figure 4.11: Ebullition emissions v/s NH_4.

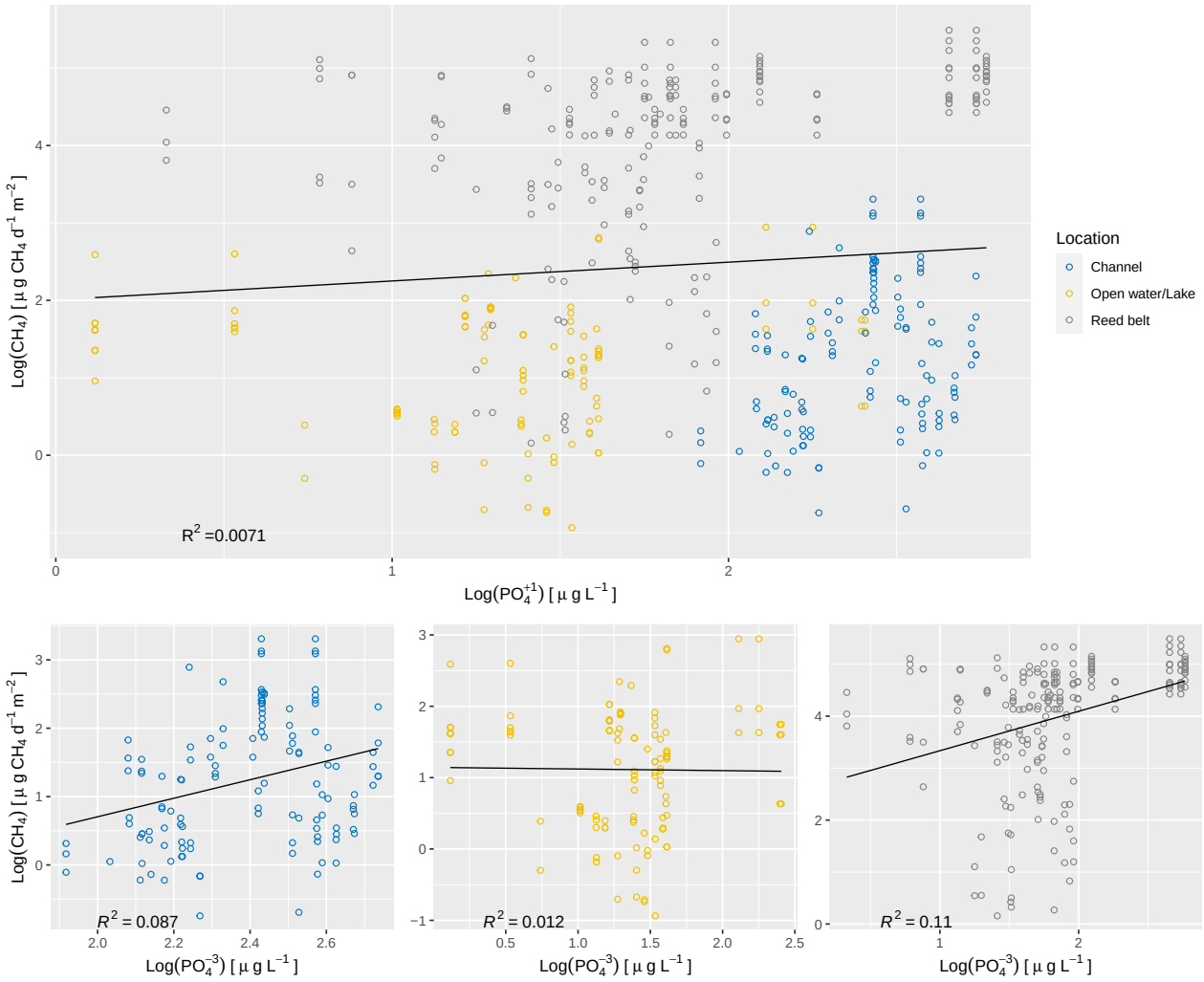

Figure 4.12: Ebullition emissions v/s PO_4.

Regarding carbon content, correlation was high for *NPOC* and moderate for *IC* when looking at the whole data, with R^2 = 0.75 and 0.42, respectively (see Figures 4.13 and 4.14). Both interactions were positive, which would drive to conclude that when there is more carbon in the water it is more likely to have more CH_4 bubbles and more concentrated. This follows the logic that a higher carbon availability might result in higher chances of this carbon being eventually transformed to CH_4, which is expected in a vegetated wetland with constant production and decomposition of organic matter like Lake Neusiedl.

At a local scale, for *NPOC* there was no correlation in the CH and OW (R^2 = 0.06 and 0.0022, respectively) but in the RB, where the *NPOC* concentrations were higher (Table 4.7), the correlation was moderate (R^2 = 0.42). For *IC*, the correlations were moderate in the RB, low in the CH and none in the OW, with R^2 = 0.43, 0.32 and 0.073, respectively (see Figures 4.13 and 4.14).

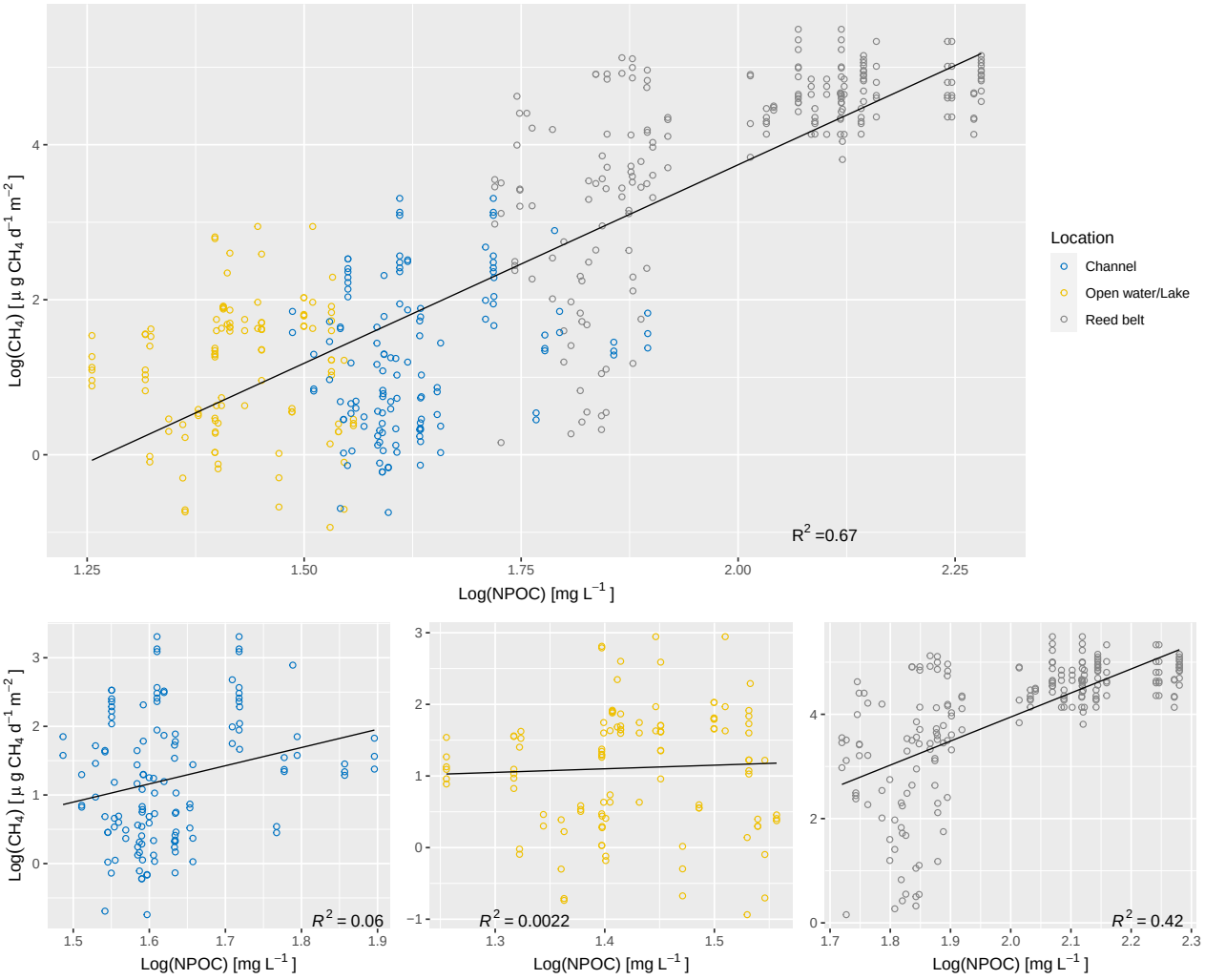

Figure 4.13: Ebullition v/s *NPOC*.

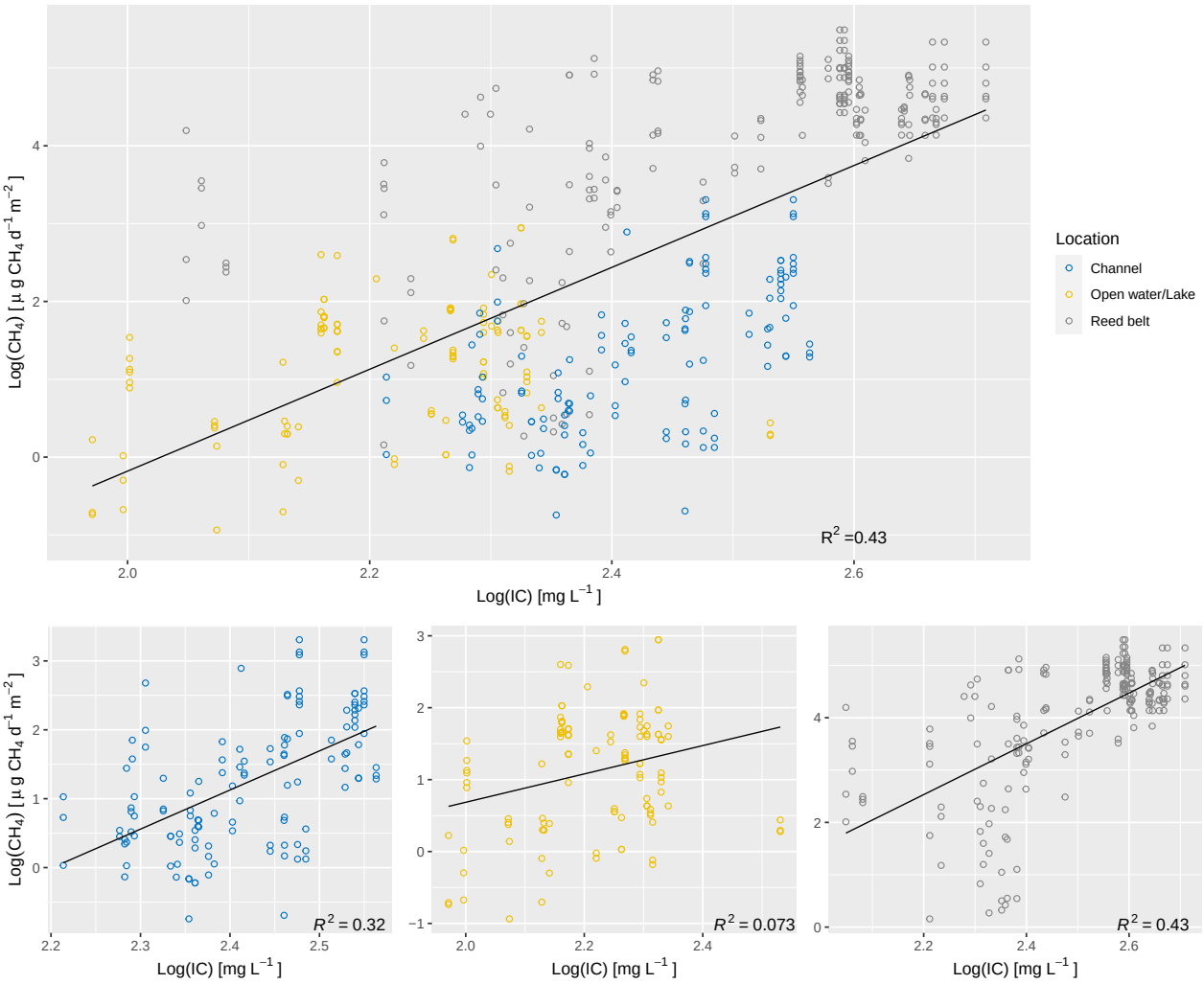

Figure 4.14: Ebullition v/s *IC*.

For in-situ parameters, daily means per location were used because the data set was smaller than the one from water samples.

$T°$ was expected to have a strong influence in CH_4 ebullition emissions because it enhances productivity, which is positively related to sediment methanogenesis rates (West *et al.*, 2016). When analyzing the overall data, R^2 was too low (0.036) but looking at each location independently (Figure 4.15), the correlation was high in the CH (R^2 = 0.65) and moderate in the OW and RB, with R^2 = 0.46 in both cases. Nevertheless, the model was too weak to be determinant.

Also *pH* showed no correlation with CH_4 ebullition rates when comparing the complete data set (R^2 = 0.0077). Locally, the correlation was moderate in the RB with R^2 = 0.53, low in the CH with R^2 = 0.2 and none in the OW with R^2 = 0.000048, where the highest pH was recorded (Table 4.2). The model was too weak to make any assumptions.

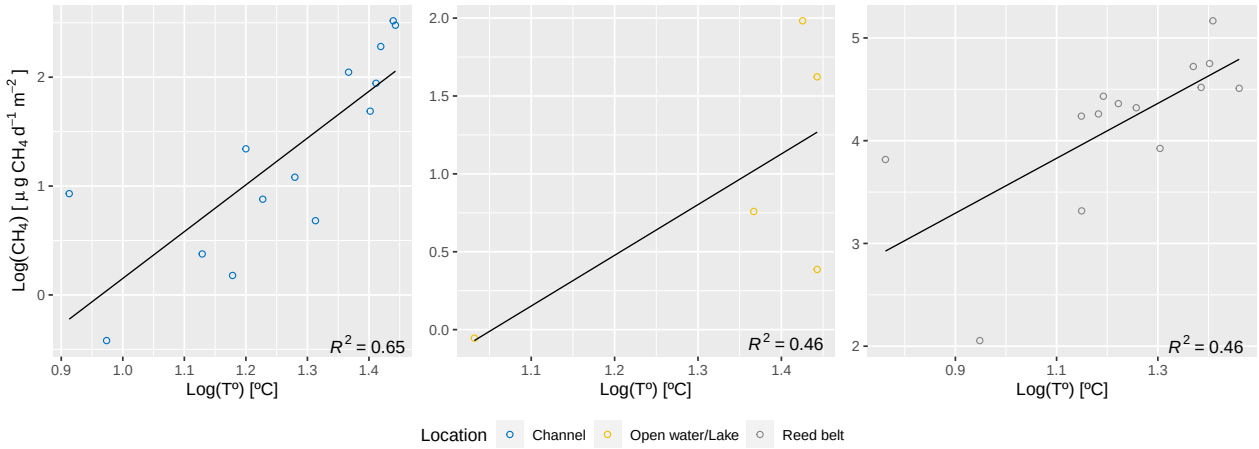

Figure 4.15: Ebullition emissions v/s $T°$.

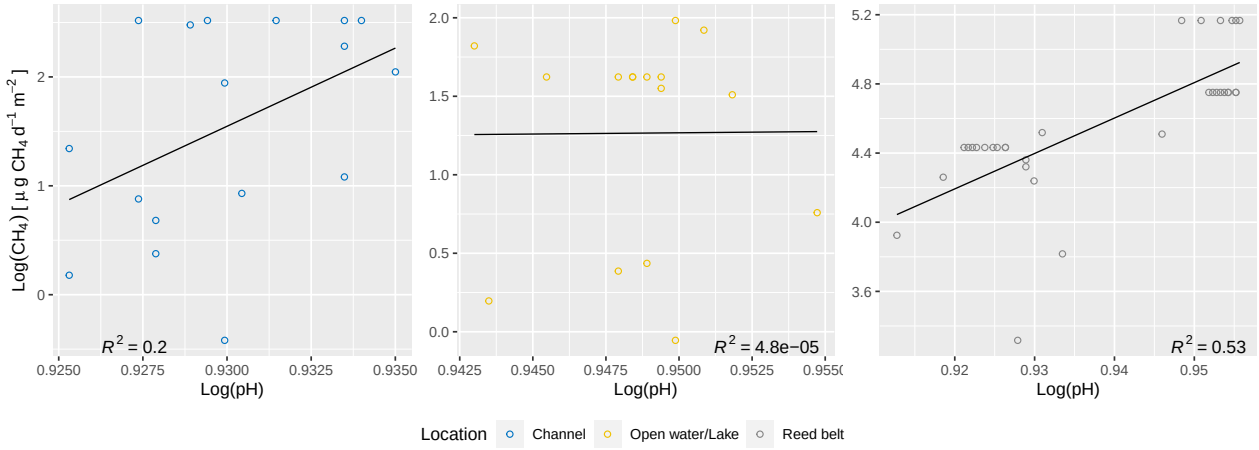

Figure 4.16: Ebullition emissions v/s pH.

The overall relation between EC and CH_4 ebullition emissions was high ($R^2 = 0.64$) when a logarithmic regression was used. The relation at the location scale was also positive, particularly high in the CH with $R^2 = 0.72$, moderate in the RB with $R^2 = 0.36$ and none in the OW ($R^2 = 0.013$). In general, it could be stated that the higher the EC, the higher the CH_4 ebullition emission rates (see Figure 4.17).

Redox potential had low correlation with CH_4 ebullition rates when all data was compared ($R^2 = 0.27$). When locations were compared separately, the relation in the CH was high with $R^2 = 0.6$, moderate in the RB with $R^2 = 0.34$ and none in the OW with $R^2 = 0.13$. All relations were negative, which implies that the lower the redox (or the more negative), the higher or the more concentrated are the CH_4 ebullition emissions (see Figure 4.18). This is coherent with what is known about methanogenesis occurring when all other electron acceptors have been used up, normally occurring at deeper anaerobic layers of the sediments with very low redox potential. It is interesting to observe the same principle in this water column, where the methanogenesis is almost impossible to occur.

Finally, the depth of the water column was negatively correlated with CH_4 ebullition rates (see Figure 4.19). Using the overall data a $R^2 = 0.8$ was obtained, however, it is important to notice that there were important differences between water depth in the RB in comparison with the OW and CH (see Table 4.3), therefore, the model did not consider values in between. Using

the specific location data R^2 = 0.66, 0.41 and 0.17 were obtained for CH, RB and OW, respectively. This result suggests that a decrease of the water level would result in an increase of the CH_4 ebullition concentrations, which is exactly what happened during the monitoring period as a consequence of the increase in $T°$ and also what has been observed by Torres-Alvarado *et al.* (2005).

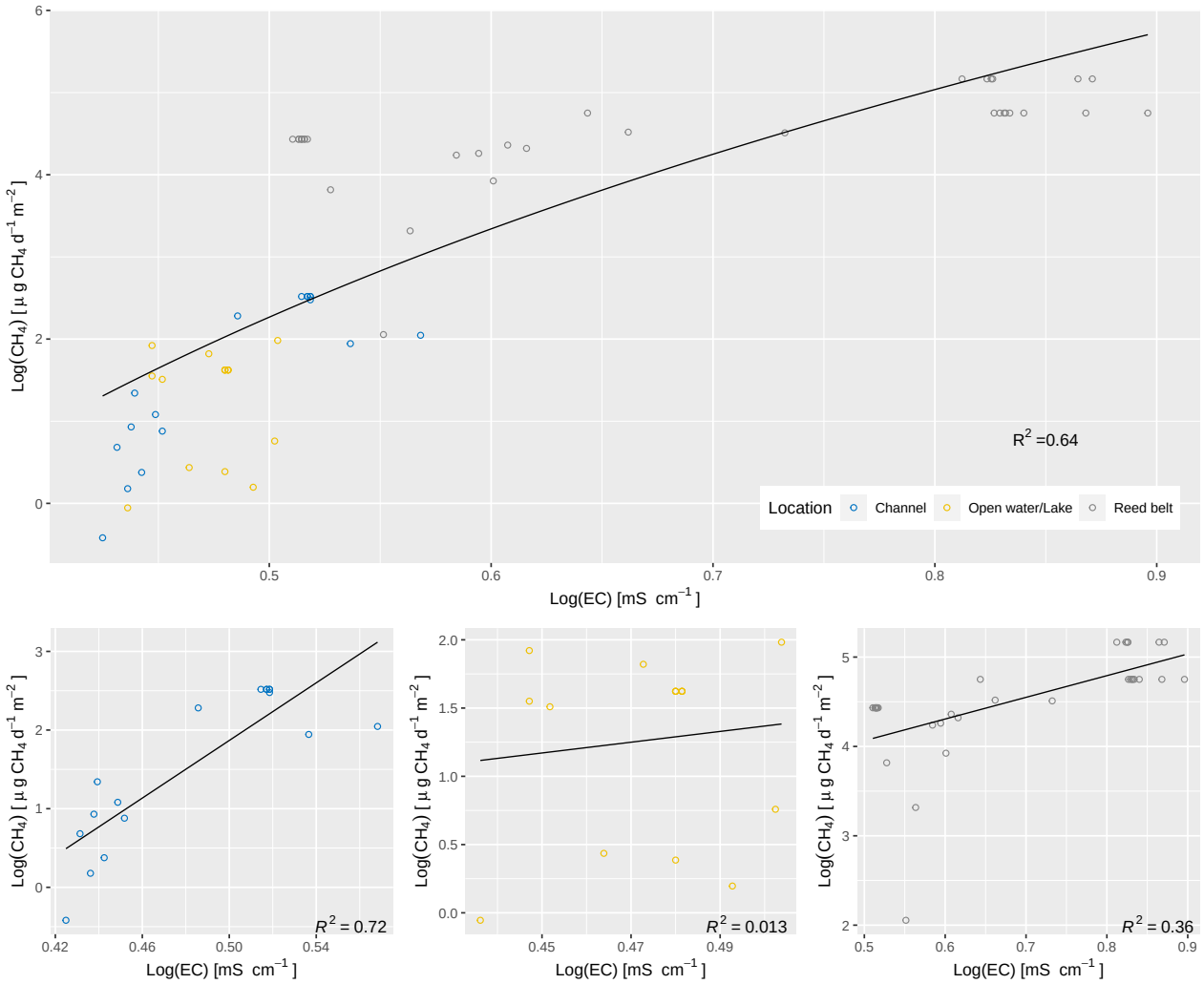

Figure 4.17: Ebullition v/s *EC*.

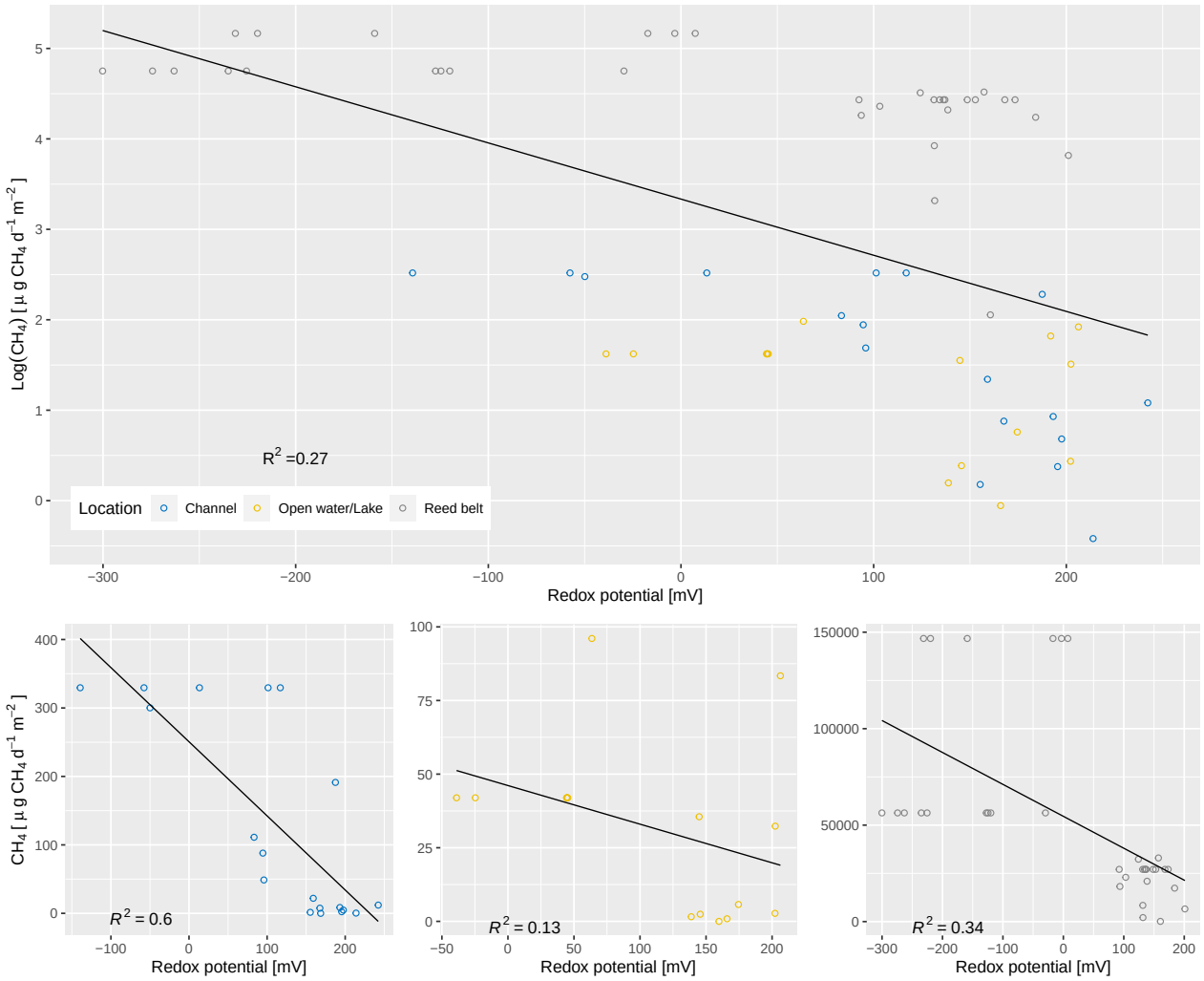

Figure 4.18: Ebullition v/s redox potential.

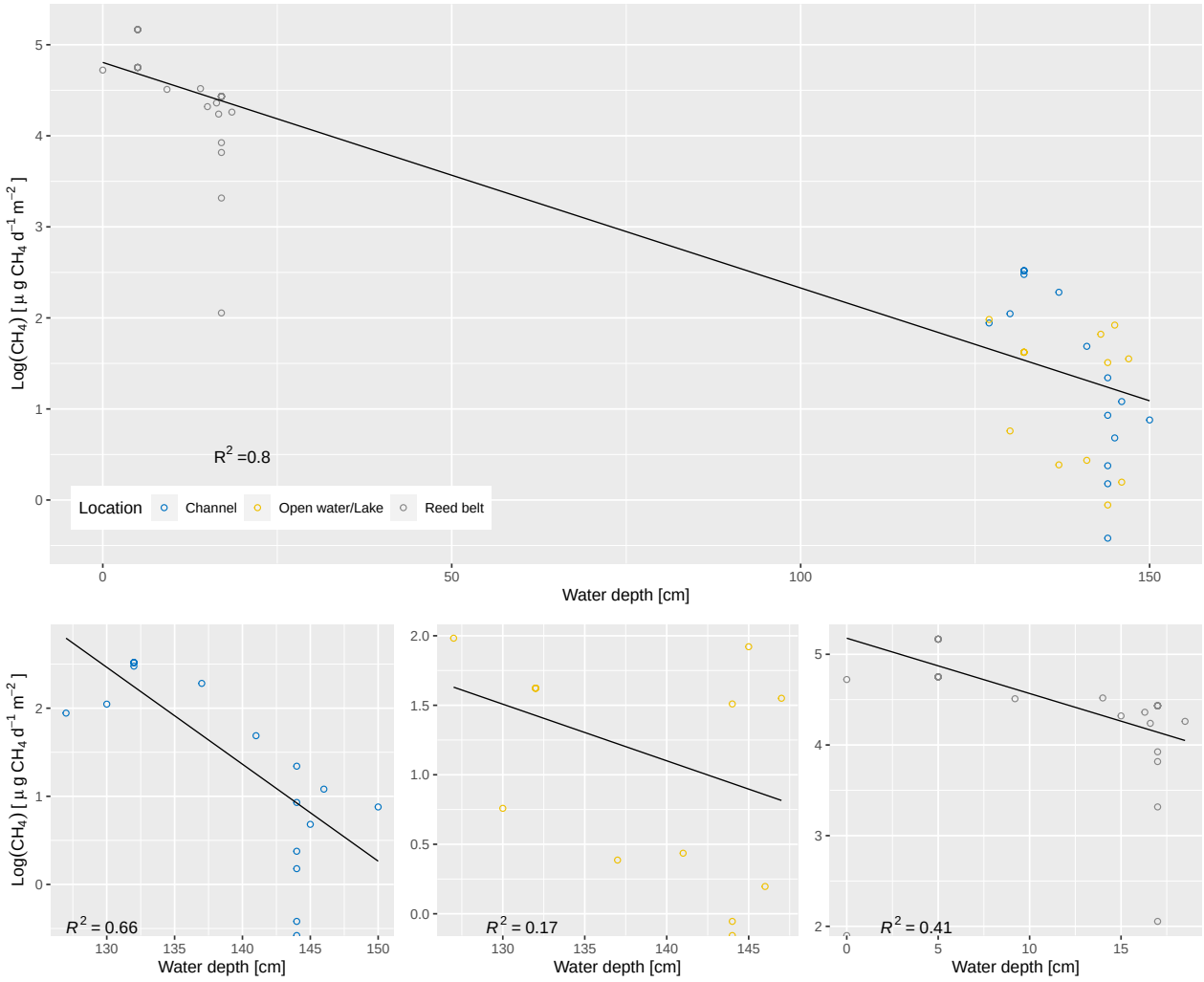

Figure 4.19: Ebullition v/s water depth.

4.4.3 CH_4 diffusion

CH_4 diffusion was estimated from in-situ chamber measurements. The results are given in $mg\ CH_4\ m^{-2}h^{-1}$ and compared with the ebullition emissions transformed to the same units. Mean values are summarized in Table 4.10.

Table 4.10: Diffusion v/s Ebullition.

Location	**CH_4 diffusion rate** $[\frac{mg}{m^2h}]$	**CH_4 ebullition rate** $[\frac{mg}{m^2h}]$
Channel	0.26	0.004
Open water/Lake	0.33	0.002
Reed belt	0.43	1.419

During the measurement period, diffusion was much more significant (two orders of magnitude higher) than ebullition in the CH and OW but in the RB ebullition was three times higher than diffusion. Diffusion in the CH was the lowest in between locations but for ebullition the OW was the lowest of them. The RB was in both cases the one with the highest rate.

From these results, it can be assumed that the reed plays an important role in CH_4 emissions, specially for the ebullition pathway. The sediments around vegetation might be more productive because of the organic material available and the high amounts of organic N present, which could eventually enhance CH_4 production. Moreover, the presence of the reed and the low water level could also contribute with pore space and conditions for the accumulation of this CH_4 in form of bubbles and later release to the atmosphere. In shallow waters the sediments in the bottom of the lake are more exposed and closer to the atmosphere where sudden changes in air pressure could trigger the release of bubbles. Particularly, the drier the RB became, the hotter and the less oxygenated this part of the lake was, which coincided with the higher CH_4 ebullition emissions. The OW and CH were probably too deep to have atmospheric pressure changes influencing ebullition emissions.

In the OW, CH_4 diffusion emissions were, in average, 27 % higher than in the CH. These two locations had similar water depth but oxygen levels were higher in the OW most of the time. Taking into account the strong winds that exist in the area, specially in open water areas that are not protected by the reed, wind might be considered as an important physical driver to diffusion emissions in the OW because of its contribution to water mixing. Regarding ebullition emissions, T° and EC should be taken into account. In the CH, CH_4 ebullition emissions were, in average, 50 % higher than in the OW, while T° and EC were, in average, also higher in the CH than in the OW, which would confirm a possitive interaction between CH_4 ebullition and these parameters. Another point to highlight is the differences in the lake bed of these two locations. Water samples analysis indicated that the OW had more inorganic content but it was also noticeable to the eye that there was no vegetation cover as there was in the CH, probably because of the turbidity caused by the wind in this open area. This could negatively influence ebullition.

Looking at Table 4.10, there is an evident heterogeneity in terms of CH_4 emissions. Just studying three locations of the lake, not too far away from each other, it was possible to observe the great influence of the lake characteristics on the CH_4 emission rates, particularly affecting

the ebullition pathway.

4.4.4 CO_2 and N_2O ebullition emissions

CO_2 and N_2O were also measured from the samples collected from the ebullition traps. Mean daily values are shown in Figures 4.20 and 4.21, and summarized in Table 4.11.

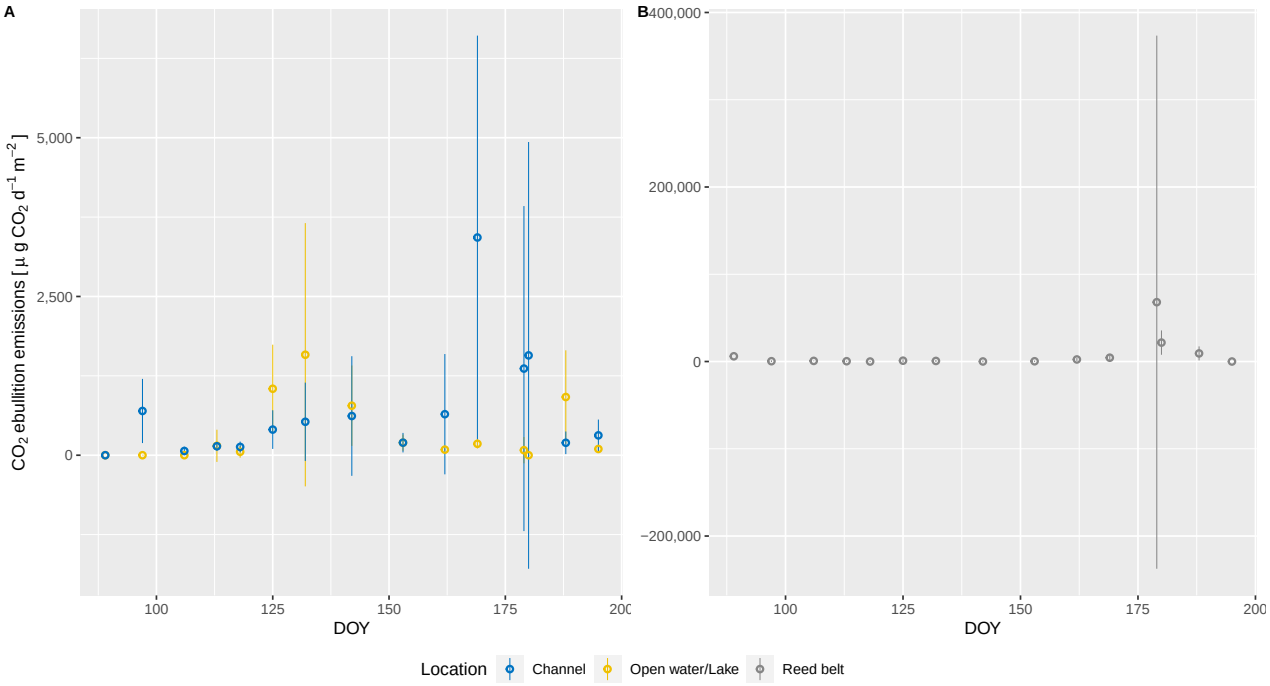

Figure 4.20: CO_2 ebullition emissions with their SD in A: CH and OW, and B: RB.

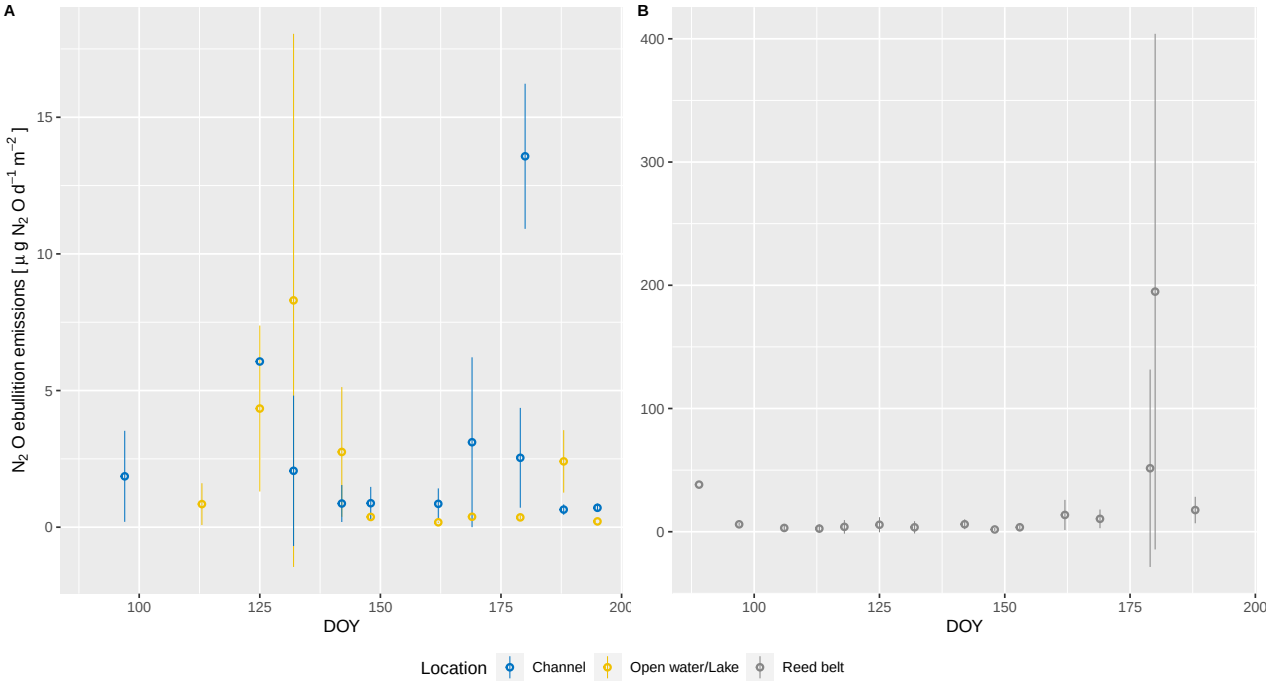

Figure 4.21: N_2O ebullition emissions with their SD in A: CH and OW, and B: RB.

Table 4.11: Mean daily CO_2, N_2O and CH_4 ebullition concentrations and emissions with their SD. The ratio $CH_4 : CO_2$ was calculated from emission rates.

Location	**CO_2** [ppm]	**CO_2** [$\frac{\mu g}{m^2 d}$]	**N_2O** [ppm]	**N_2O** [$\frac{\mu g}{m^2 d}$]	**CH_4** [ppm]	**CH_4** [$\frac{\mu g}{m^2 d}$]	**$CH_4 : CO_2$**
Channel	4 413.1	839.5	9.8	1.13	1 034.9	6 154.5	7.33
Open water/Lake	2 416.8	653.2	4.2	2.03	937.9	7 909.5	12.11
Reed belt	23 440.3	901.0	110.0	12.50	204 211.5	10 205.7	11.33

It was observed that, in average, CO_2 ebullition concentration from the CH samples was about 4 times higher than CH_4 ebullition concentration and 2.5 times higher in the OW. It was a different case in the RB where mean CH_4 ebullition concentration was almost 9 times higher than mean CO_2 ebullition concentration (see results in Annexes, chapter B.2). When fluxes were compared, these relationships changed because the molar weights of molecules were considered (CH_4 = 16.04 g/mol and CO_2 = 44.01 g/mol). In this case, CH_4 fluxes were always much greater than CO_2 fluxes, about 7, 11 and 12 times higher in the CH, RB and OW, respectively. This agrees with what was observed by Soja *et al.* (2014), who established that ebullition in Lake Neusiedl contains mostly CH_4 and a very small amount of CO_2 because at high pH (8.5-9.0) HCO_3 and CO_3^{-2} are more stable than CO_2. In order to further analyze the $CH_4 : CO_2$ flux ratio, Figure 4.22 illustrates how its variation over time.

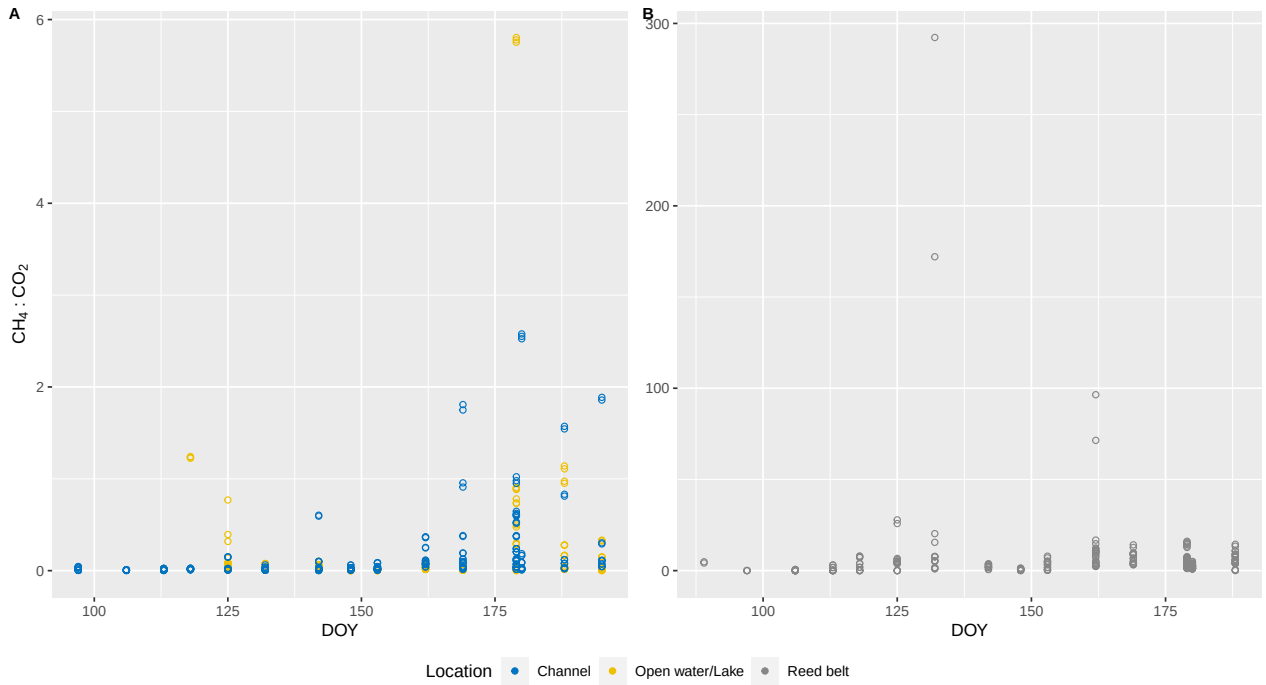

Figure 4.22: $CH_4 : CO_2$ flux ratio in A: CH and OW, and B: RB.

Changes in the $CH_4 : CO_2$ ratio sheds lights about the CH_4 production/consumption rate. If the ratio increses, methane oxidation is probably decreasing or CO_2 is being consumed by methanogens on a higher rate. In Figure 4.22 it is possible to observe in the OW and RB the two peaks also observed in $T°$ and all the measured GHGs.

Mean N_2O concentrations and fluxes were much lower than CO_2 and CH_4 in all locations. In general, when NH_4^+ loads are low, nitrification and denitrification do not play an important role, therefore, little N_2O is produced (Soja *et al.*, 2014).

Chapter 5

Conclusions

The study's aims of quantifying CH_4 ebullition emissions in Lake Neusiedl and understanding its potential relationship with water quality parameters was successfully achieved.

Mean ebullition emission rates were estimated as 50.2, 85.1 and 34 064.6 $\mu g\ CH_4\ m^{-2}d^{-1}$ in the OW, CH and RB, respectively. The parameters that proved to have the highest correlation with CH_4 ebullition emissions when considered as a single factor (complete data set from all locations) were water depth (R^2=0.80), $NPOC$ (R^2=0.67), EC (R^2=0.64), TN (R^2=0.57), and IC (R^2=0.43). The only parameter that demonstrated to have moderate to high correlation with CH_4 ebullition emissions when looking at each location separately was $T°$. Redox potential, water depth, EC and pH indicated also low to high correlation but only in the CH and RB.

For all nutrients and carbon concentrations, except for NH_4^+, there are significant differences between some or all locations. Regarding to CH_4 ebullition emissions, there are significant differences between the RB and the other two, but not between OW and CH. Great variability of CH_4 emissions were observed in time, for volume, concentration and flux amounts in all locations. Thus, spatial and temporal heterogeneity in Lake Neusiedl was confirmed. Nonetheles, models were too weak to prove any correlation between nutrients and CH_4 ebullition emissions.

Mean diffusion emission rates were estimated as 6 154.5, 7 909.5 and 10 205.7 $\mu g\ CH_4\ m^{-2}d^{-1}$ in the CH, OW and RB, respectively. Mean CO_2 ebullition rates were estimated as 839.5, 653.2 and 901.0 $\mu g\ CH_4\ m^{-2}d^{-1}$ in the CH, OW and RB, respectively. Mean N_2O ebullition rates were estimated as 1.1, 2.0 and 12.5 $\mu g\ CH_4\ m^{-2}d^{-1}$ in the CH, OW and RB, respectively.

It is important to highlight that all parameters analyzed in this study were measured from samples collected in the water column which is not a direct indicator of what is occurring in the sediments where the methanogenesis should be happening. Nevertheless, there is a constant interaction that needs to be better understood in order to identify the primary drivers of CH_4 ebullition emissions.

The challenges of working in the field are that parameters cannot be isolated or altered, they constantly interact with each other and that conditions might not be ideal for comparison. It has been previously stated that the highest CH_4 emissions rates had been recorded in late summer and early autumn due to greater availability of degradable organic matter accumulated from dead plants and warm temperatures that enhance biotransformation (Soja *et al.*, 2014). There-

fore, this study could be pursued by a longer observation period extended towards autumn. In this case, the RB location would have to be placed where there is still water by that time. It is also suggested to include a location where nutrients loads are higher, for example, closer to the sewage treatment plant in the other side of the lake or residential buildings were anthropogenic impacts could be also evaluated. Another alternative would be to measure nutrients concentrations directly within the sediments layer.

Bibliography

Bastviken, D., Cole, J., Pace, M., & Tranvik, L. 2004. Methane emissions from lakes: Dependence of lake characteristics, two regional assessments, and a global estimate. *Global biogeochemical cycles*, **18**(4).

Benoit, K. 2011. Linear regression models with logarithmic transformations. *London School of Economics, London*, **22**(1), 23–36.

Boguski, T. K. 2006. Understanding units of measurement. *Environmental science and technology briefs for citizens*.

Burke, S. A., Wik, M., Lang, A., Contosta, A. R., Palace, M., Crill, P. M., & Varner, R. K. 2019. Long-term measurements of methane ebullition from thaw ponds. *Journal of Geophysical Research: Biogeosciences*, **124**(7), 2208–2221.

Cao, M., Gregson, K., & Marshall, S. 1998. Global methane emission from wetlands and its sensitivity to climate change. *Atmospheric environment*, **32**(19), 3293–3299.

Davidson, T. A., Audet, J., Svenning, J. C., Lauridsen, T. L., Søndergaard, M., Landkildehus, F., Larsen, S. E., & Jeppesen, E. 2015. Eutrophication effects on greenhouse gas fluxes from shallow-lake mesocosms override those of climate warming. *Global Change Biology*, **21**(12), 4449–4463.

Davidson, T. A., Audet, J., Jeppesen, E., Landkildehus, F., Lauridsen, T. L., Søndergaard, M., & Syväranta, J. 2018. Synergy between nutrients and warming enhances methane ebullition from experimental lakes. *Nature Climate Change*, **8**(2), 156–160.

DelSontro, T., Boutet, L., St-Pierre, A., del Giorgio, P. A., & Prairie, Y. T. 2016. Methane ebullition and diffusion from northern ponds and lakes regulated by the interaction between temperature and system productivity. *Limnology and Oceanography*, **61**(S1), S62–S77.

Dinka, M., Ágoston Szabó, E., & Szeglet, P. 2010. Comparison between biomass and C, N, P, S contents of vigorous and die-back reed stands of Lake Fertő/Neusiedler See. *Biologia*, **65**(2), 237–247.

Gardolinski, P. C., Hanrahan, G., Achterberg, E. P., Gledhill, M., Tappin, A. D., House, W. A., & Worsfold, P. J. 2001. Comparison of sample storage protocols for the determination of nutrients in natural waters. *Water Research*, **35**(15), 3670–3678.

Gholikandi, G. B., & Sadabad, H. R. 2014. Methanogenesis: biochemistry, ecological functions, natural and engineered environments. *Nova Science Publishers, Incorporated*.

Kandeler, E., & Gerber, H. 1988. Short-term assay of soil urease activity using colorimetric determination of ammonium. *Biology and fertility of Soils*, **6**(1), 68–72.

Klüber, H. D., & Conrad, R. 1998. Effects of nitrate, nitrite, NO and N2O on methanogenesis and other redox processes in anoxic rice field soil. *FEMS Microbiology Ecology*, **25**(3), 301–318.

Lovley, D. R., & Phillips, E. J. 1987. Competitive mechanisms for inhibition of sulfate reduction and methane production in the zone of ferric iron reduction in sediments. *Applied and Environmental Microbiology*, **53**(11), 2636–2641.

Magyar, N., Hatvani, I. G., Székely, I. K., Herzig, A., Dinka, M., & Kovács, J. 2013. Application of multivariate statistical methods in determining spatial changes in water quality in the Austrian part of Neusiedler See. *Ecological Engineering*, **55**, 82–92.

Miranda, K. M., Espey, M. G., & Wink, D. A. 2001. A rapid, simple spectrophotometric method for simultaneous detection of nitrate and nitrite. *Nitric oxide*, **5**(1), 62–71.

Murphy, J. A. M. E. S., & Riley, J. P. 1962. A modified single solution method for the determination of phosphate in natural waters. *Analytica chimica acta*, **27**, 31–36.

Pihlatie, M. K., Christiansen, J. R., Aaltonen, H., Korhonen, J. F., Nordbo, A., Rasilo, T., ..., & Pumpanen, J. 2013. Comparison of static chambers to measure CH4 emissions from soils. *Agricultural and forest meteorology*, **171**, 124–136.

Rantakari, M., & Kortelainen, P. 2008. Controls of organic and inorganic carbon in randomly selected Boreal lakes in varied catchments. *Biogeochemistry*, **91**(2), 151–162.

Sanches, L. F., Guenet, B., Marinho, C. C., Barros, N., & de Assis Esteves, F. 2019. Global regulation of methane emission from natural lakes. *Scientific Reports*, **9**(1), 1–10.

Schranz, L. M. 2016. The protection of lakes in the face of climate change challenges regarding the preservation of the" good water status": Explained on the examples of Lake Constance and Lake Neusiedl. *Doctoral dissertation, Wien*.

Segers, R. 1998. Methane production and methane consumption: a review of processes underlying wetland methane fluxes. *Biogeochemistry*, **41**(1), 23–51.

Soja, G., Züger, J., Knoflacher, M., Kinner, P., & Soja, A. M. 2013. Climate impacts on water balance of a shallow steppe lake in Eastern Austria (Lake Neusiedl). *Journal of Hydrology*, **480**, 115–124.

Soja, G., Kitzler, B., & Soja, A. M. 2014. Emissions of greenhouse gases from Lake Neusiedl, a shallow steppe lake in Eastern Austria. *Hydrobiologia*, **731**(1), 125–138.

Torres-Alvarado, R., Ramírez-Vives, F., Fernández, F. J., & Barriga-Sosa, I. 2005. Methanogenesis and methane oxidation in wetlands: implications in the global carbon cycle. *Hidrobiológica*, **15**(3), 327–349.

Tranvik, L. J., Downing, J. A., Cotner, J. B., Loiselle, S. A., Striegl, R. G., Ballatore, T. J., ..., & Weyhenmeyer, G. A. 2009. Lakes and reservoirs as regulators of carbon cycling and climate. *Limnology and Oceanography*, **54**(6part2), 2298–2314.

Watson, A., & Nedwell, D. B. 1998. Methane production and emission from peat: the influence of anions (sulphate, nitrate) from acid rain. *Atmospheric Environment*, **32**(19), 3239–3245.

West, W. E., Creamer, K. P., & Jones, S. E. 2016. Productivity and depth regulate lake contributions to atmospheric methane. *Limnology and Oceanography*, **61**, S51–S61.

Whalen, S. C. 2005. Biogeochemistry of methane exchange between natural wetlands and the atmosphere. *Environmental Engineering Science*, **22**(1), 73–94.

Wik, M., Thornton, B. F., Bastviken, D., Uhlbäck, J., & Crill, P. M. 2016. Biased sampling of methane release from northern lakes: A problem for extrapolation. *Geophysical Research Letters*, **43**(3), 1256–1262.

Worsfold, P. J., Gimbert, L. J., Mankasingh, U., Omaka, O. N., Hanrahan, G., Gardolinski, P. C., Haygarthd, P. M., Turnere, B. L., Keith-Roach, M. J., & McKelvie, I. D. 2005. Sampling, sample treatment and quality assurance issues for the determination of phosphorus species in natural waters and soils. *Talanta*, **66**(2), 273–293.

Wuebbles, D. J., & Hayhoe, K. 2002. Atmospheric methane and global change. *Earth-Science Reviews*, **57**(3-4), 117–210.

Annexes

Appendix A

Materials, instruments and equipment, and chemicals lists

A.1 Field work

A.1.1 Materials

On a daily basis, the following materials were used on the field:

- Water
  - Braun Omnifix 50 *ml* plastic syringes
  - Terumo Agani sterile needles
  - Macherey-Nagel filter papers MN 619 G $1/4$ $\varnothing 125$ *mm*
  - Macherey-Nagel Chromafil Xtra PET 0.45 μm disposable syringe filter
  - 20 *ml* plastic bottles
  - 500 *ml* plastic beakers
  - 235 *mm* hdpe funnels
  - Cooler box and ice packs
- Gas
  - 20 *ml* pre-vacuumed glass vials
  - Macherey-Nagel rubber septums and aluminum crimp caps

A.1.2 Instruments and equipment

On a daily basis, the following instruments and equipment were used on the field:

- Water
  - HOBO temperature data loggers
  - WTW portable multi-parameter analyzer with $T°$, pH, EC, DO and redox sensors.
- Gas
  - Los Gatos mobile gas analyzer (when available)

A.2 Lab work

A.2.1 Materials

On a daily basis, the following materials were used in the lab:

- Water
  - Eppendorf pippets and multipippets
  - Eppendorf tips and combitips
  - Glass pippetes
  - 96-well polystyrene, flat bottom microtiter plates
  - Volumetric flasks
  - Glass flasks
  - Eppendorf 1.5-2 *ml* plastic vials
  - Spatulas
  - High purity deionized water (Milli-Q)
- Gas
  - Braun Omnifix 50 *ml* plastic syringes
  - Hamilton 500 *ml* acrylic syringe model S-500
  - Hamilton 1 *ml* glass syringe (air tight)
  - Messer N_2 6.0 standard gas
  - Restek 1 *L* multi-layer polypropylene gas bag

A.2.2 Instruments and equipment

On a daily basis, the following instruments and equipment were used in the lab:

- Water
  - Nano Quant UV-VIS infinite M200PRO
  - Vortex-genie 2 stirrer
  - Labnet mini incubator
  - Kern ADB analytical balance
- Gas
  - Picarro G2201-i analyzer
  - Agilent Technologies 7890B gas chromatography system with a 7697A head-space sampler

A.2.3 Chemicals

For NO_3^{-2}, NH_4^+ and PO_4^{-3} colorimetric determination, the following chemicals were necessary:

- NO_3^{-2}
  - Vanadium (III) chloride
  - N-napthylethylenediamine dihydrochloride
  - Sulfanilamide
  - Potassium nitrate
  - Hydrochloric acid
- NH_4^+
  - Sodium hydroxide
  - Sodium salicylate
  - Sodium nitroprusside dihydrate
  - Dichloroisocyanuric acid sodium salt dihydrate
  - Ammonium chloride
- PO_4^{-3}
  - Ammonium heptamolybdate tetrahydrate
  - Potassium antimony (III)oxide tartrate sesquihydrate
  - Sulfuric acid 95-97 %
  - Ascorbic acid
  - Potassium dihydrogen phosphate

Appendix B

Other results

B.1 Bubbles' CH_4 concentration

CH_4 ebullition concentrations with their SD are shown in Figures B.1 and B.2. Plots include all locations measured with Picarro and GC instruments.

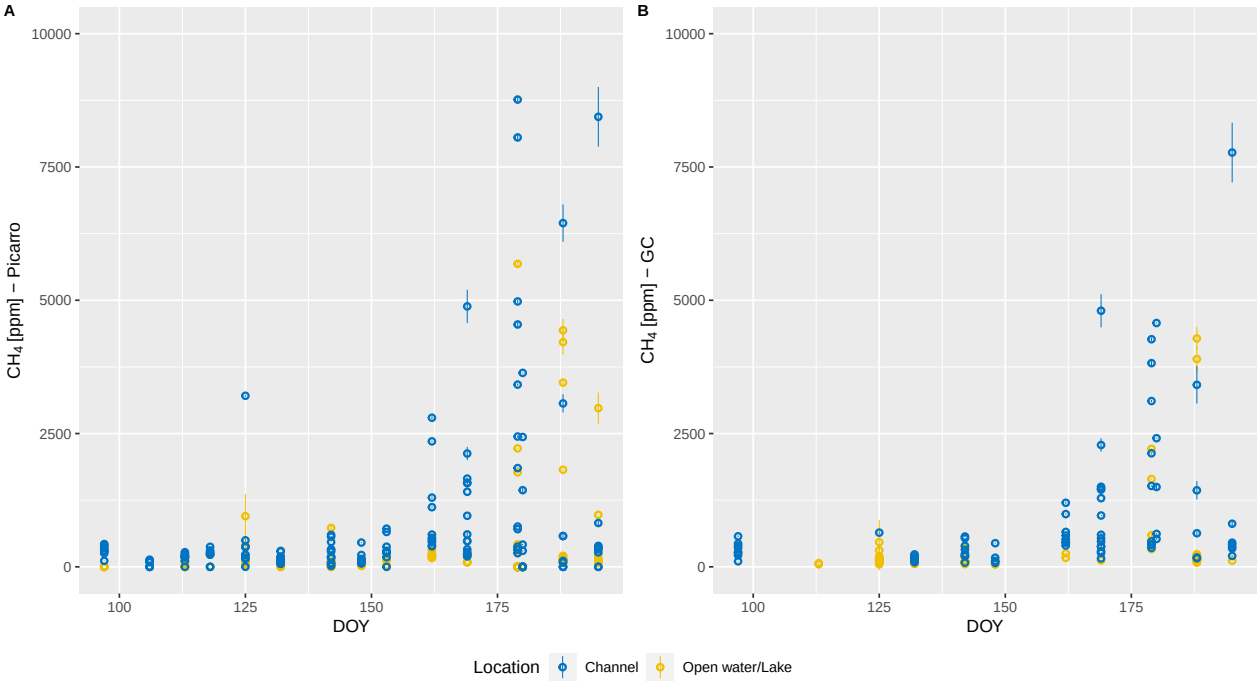

Figure B.1: CH_4 ebullition concentrations with their SD in CH and OW, measured with A: Picarro and B: GC.

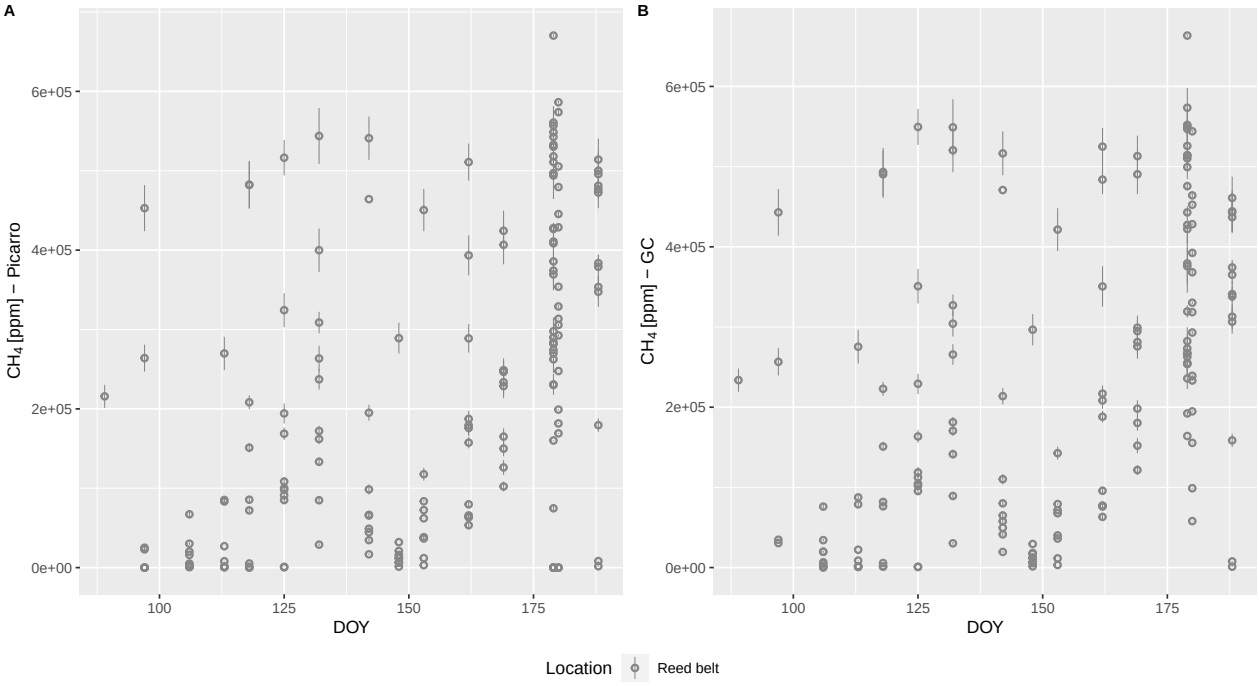

Figure B.2: CH_4 ebullition concentrations with their SD in RB, measured with A: Picarro and B: GC.

B.2 Bubbles' CO_2 and N_2O concentrations

CO_2 and N_2O ebullition concentrations with their SD are shown in Figures B.3 and B.4.

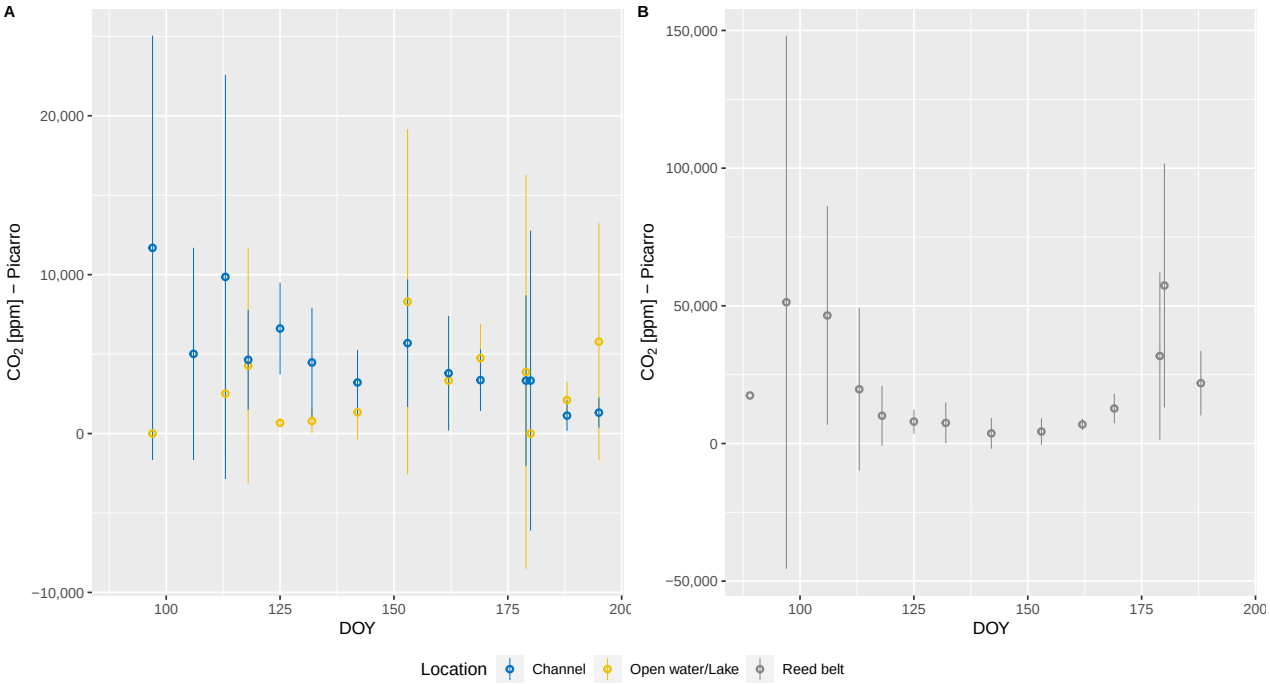

Figure B.3: CO_2 ebullition emissions in A: CH and OW, and B: RB.

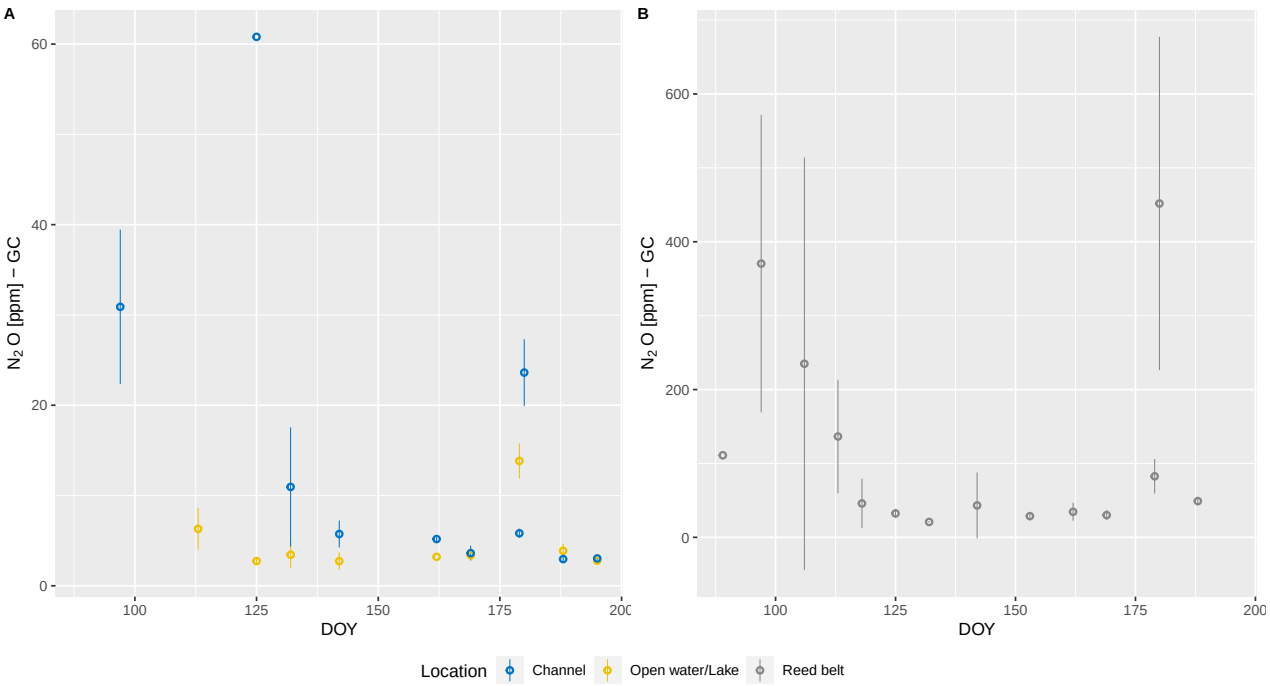

Figure B.4: N_2O ebullition emissions in A: CH and OW, and B: RB.